PhD Thesis

Energy management strategy for a solar race car including meteorologic and probabilistic variables

Student
Esteban Betancur Valencia

Responsible professor
Gilberto Osorio-Gómez

Grupo de Investigación en Ingeniería de Diseño - GRID
Department of Product Design Engineering
Universidad EAFIT
Medellín

November, 2018

Abstract

This thesis describes the energy management strategy for racing solar cars, the racing strategy is treated as an optimal control problem with random variables and uncertain predictions. A computational model is developed for estimating the vehicle performance under specific circumstances. Two evolutionary heuristic optimization methods are implemented and tested for this case, their effectiveness, convergence and efficiency is measured and compared to exhaustive search approaches. The dependency on solar radiation is validated using the computational model with different test cases. In order to reduce the uncertainties on the solar radiation estimation, satellite images are used as inputs to image processing and machine learning techniques, their efficacy is compared. Finally, a validation case is executed and different scenarios are evaluated with the inclusion of the proposed methods, the experimental performance of a vehicle obtained using the strategy in the World Solar Challenge 2015 is exposed and compared to the predicted results from the simulation.

Keywords: Solar Car, Race strategy, Energy management, Heuristic optimization, Solar resource.

Contents

List of Abbreviations

The different abbreviations, acronyms and symbols used repeatedly throughout the thesis are listed and defined in the table below, arranged by order of appearance within the document.

CO_2 .... Carbon Dioxide particles
WSC .... Bridgestone World Solar Challenge
ESC .... European Solar Challenge
ASC .... American Solar Challenge
GA .... Genetic Algorithms optimization method
DP .... Dynamic Programming
BB-BC ...... Big Bang-Big Crunch optimization method
W/m^2 .... Watts per square meter
GHI .... Global Horizontal Irradiance
RMSE .... Root-Mean-Square Error
K_c .... Clear Sky Index
GHI_{clr} .... Clear Sky GHI
nRMSE ...... Normalized Root-Mean-Square Error
ANN .... Artificial Neural Network
MP .... Multilayer Perceptrons
ES .... Exhaustive Search
LS .... Local Search
SOC .... State Of Charge
CNN .... Convolutional Neural Network
HSV .... Hue-Saturation-Value color format
RGB .... Red-Green-Blue color format
MBE .... Mean Bias Error
ClrSky .... Clear Sky GHI
SClrSky ...... Scaled Clear Sky GHI

Introduction

The current growth of world population, the high rate of consumption of different resources and the environmental degradation, generate the necessity of seeking sustainable ideas and solutions for different human activities. The well-known renewable energy sources, specially the solar and wind, are gaining field on the global energy market with an annual growth of more than twice the rate of energy demand for the past 10 years (REN21 [2017]). On the other hand, the second sector with major participation on the CO_2 emissions from fuel combustion is the transportation (25%), according to the 2015 data presented by International Energy Agency (IEA [2017]).

Electric vehicles present a solution to the CO_2 emission problem on the road transport only if the electric energy source is based on renewable energies. If this condition does not happen, the real gain depends on the overall efficiency improvement and the emitting source is just transferred from the vehicle to the generation plant. In order to guarantee real zero emissions and energy autonomy, solar cars bring the proposal of having electric vehicles with an integrated solar panel acting as its main energy source. This way, the vehicle is obtaining energy from the sun while moving or parking under sunlight, Figure 1 illustrates the main components of the vehicle. During the last three decades, different competitions have been developed around the world to compare different solar vehicle prototypes presented by university-company partnerships.

The solar vehicles main feature is their energy efficiency. According to the low energy captured by the solar panel, very low consumption might be achieved while travelling in order to guarantee their energy autonomy. The vehicle effectiveness is achieved with high efficiency drivetrains and batteries, aerodynamic design, low weight components, among other issues (see Minak et al. [2017], Tamura [2016], Paterson et al. [2016], Betancur et al. [2017b], Vinnichenko et al. [2014]). In addition to the above, a clever driving speed should be imposed to the vehicle in order to optimize its performance according to its limited energy storage and collection. The vehicle energy planning on a given path is defined as energy management strategy. In most cases, this strategy is resumed on defining the velocity of the vehicle according to a desired objective function, nevertheless, other optimization variables may include certain vehicle design parameters, charging duration or number of occupants during the race.

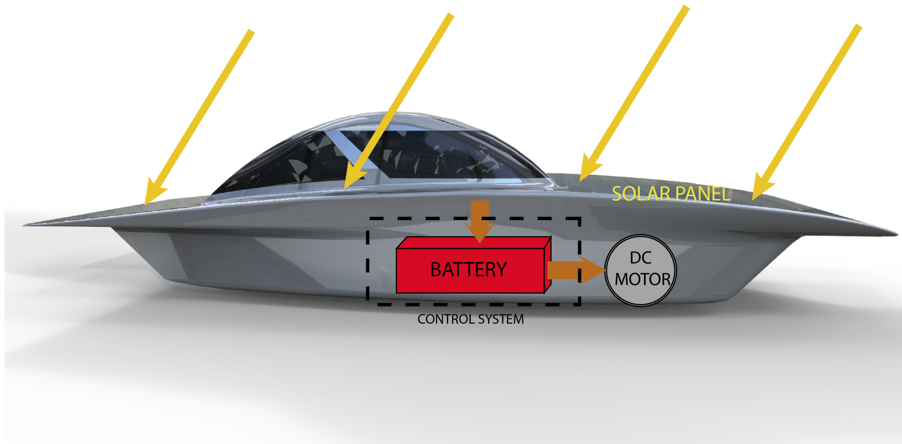

Figure 1: Solar car main components. The principal energy source is the solar panel, although it may also be charged connected to the grid as an electric vehicle.

With the necessity of defining a practical methodology to tackle the energy management optimization of racing solar cars, this thesis presents a useful solution based on the state of the art approaches of the main disciplines involved. It includes the mathematical modelling of the vehicle energy fluxes, the optimization methods and the estimation of the solar resource as the main input of the solar panel model.

The energy management strategy is, broadly speaking, the formulation of an optimization problem on which the objective function depends on the race particularities (e.g., to minimize the race time for a fixed distance or to maximize the race distance on a given time). The optimization variable is defined as the vehicle velocity, it may be time or position dependant. Therefore, an optimal velocity profile should be defined in order to optimize the vehicle performance on race, given the vehicle properties, road and predicted environmental conditions.

While executing the strategy, the real conditions may differ from the ones estimated on the initial race strategy, mainly because of unexpected road events, vehicle failures or weather variations. Although precise predictions of the race should be considered, the strategy may be recalculated several times during the race. For these "on race" recalculations an efficient and fast code is needed, in order to obtain "on time results".

The manuscript is divided in 4 chapters, each one independent of each other. To the cost of some redundancies, each chapter may be read separately. A brief description of the different chapters is given below.

Chapter 1: Background and related work

This first chapter presents the state of the art of solar car races, the energy management for land vehicles and the solar cars racing strategy. The principal solar car races are exposed and their energy management objective is defined, a difference between the races regarding the objective function is found.

The hybrid vehicles and electric trains control methods are described and compared to solar car necessities. Although the trains and hybrid vehicle models do not consider a solar input, the energy consumption is roughly equivalent.

Regarding the solar car racing strategy state of the art, a comparison between the analytic and numerical optimization methods for solar cars energy management is presented. Finally, the climate prediction for solar cars is discussed, a satellite image inclusion is recommended and image processing techniques together with machine learning procedures to estimate the solar resource are discussed.

Chapter 2: Solar car energy management: model and heuristic optimization

The computational model for simulating a solar car performance during the race is described including the energy input, consumption and storage systems. Resorting to this model, a heuristic optimization method based on genetic algorithms is proposed and its efficiency and effectiveness is compared to others reported in literature. The 2015 World Solar Challenge - WSC (World Solar Challenge [2018]) is the validation scenario for the proposed models. Different assumptions regarding the discretization of the velocity variable are also tested. A climate dependence analysis is driven through a case study of two different solar radiation scenarios, high dependency of the optimization function on this variable is demonstrated.

Chapter 3: Solar resource estimation

According to the motivation of this work, a complete chapter regarding the estimation of the energy income via solar radiation is included. This chapter provides a detailed description of the related work and proposed method to predict the energy received by the solar panel taking into account date and time, position variation and meteorological conditions.

Given the necessity of predicting the solar irradiance in different times and locations, geostationary satellite images together with the clear sky radiation are proposed as the main input to the model. Two different approaches are tested, first an image processing technique including color equalization, cloud segmentation, and cloud index estimation is implemented an tested. In the other hand, different architectures of neural networks are implemented towards a machine learning approach, satisfactory results are achieved.

Chapter 4: Solar car energy management including meteorologic and probabilistic variables

The results and conclusions from Chapters 2 and 3 are used to define the racing strategy of the vehicle "PRIMAVERA 2" from the "EPM-EAFIT Solar Car Team" on the 2015 WSC in Australia. Using the vehicle properties, a proper meteorologic estimation and considering random occurrences, a racing strategy is calculated to be followed during the race. Experimental results are exposed and explained. Although unexpected events took place, the strategy recalculation during the race proposed new solutions to minimize the racing time. Competitive results are obtained in the race due to the strategy plan.

Chapter 1

Background and related work

The content of this chapter has been partially published in Betancur et al. [2017c].

1.1 Solar car competitions

Solar cars represent engineering challenges where the main purpose is to develop a vehicle with enough efficiency to travel long distances using only solar energy. Resorting a project-based learning methodology, universities from all over the world make up solar car teams including students from different disciplines and educational levels, resulting in an efficient educational methodology, linking teaching with the professional sphere (de Los Rios et al. [2010]). Solar car races and challenges are organized for these teams to bring their proposal and test the vehicles under certain conditions. The most recognized competitions are described in the following sections.

1.1.1 World Solar Challenge - WSC

This competition is held every two years, giving the competitors enough time to design, build and test a new car for every event according to the changing regulations. The event takes place in Australia with the main objective of travelling 3022 kilometres in a maximum of 7 days between the cities of Darwin and Adelaide. To the date, three different categories are conceived in this competition: Challenger, Cruiser and Adventure (World Solar Challenge [2018]).

The Challenger class is a single-seater category where the vehicles are judged based on the total time to cover the race length using only solar energy and with limited panel and battery capacity. The first to arrive without using external energy sources is the winner. In this case the race strategy objective is to find the optimal velocity that minimizes the race time with a fixed distance and subject to different energy, road and logistic restrictions.

The Cruiser class is aimed to evaluate more "conventional" vehicles. Cars with two or more seats are judged from two different perspectives: energy efficiency in terms of people transported per energy used and practicality defined by a panel of judges, the battery size is not limited in this case. The practicality must be achieved since the design as it includes ease of access and use, style, interior space among other considerations. Regarding the energy efficiency, the race objective function is defined by the ratio between the persons carried per kilometre and the total external energy used. Therefore, a racing strategy may include the optimal estimation of the battery size, number of persons per race section, number of recharging stops and velocity.

Vehicles that do not comply with the Challenger or Cruiser regulations but still wish to join the event are assigned to Adventure class. No competition or qualification is considered for this class.

1.1.2 European Solar Challenge - ESC

The European solar challenge is a biannual event that invites different solar cars from Europe and other continents to compete on a series of challenges. The competition is done in a Formula-1 Circuit on Zolder, Belgium. Although there is not a defined division on the event, the cars can be classified as Challenger and Cruiser class according the WSC regulations (See 1.1.1).

The race event entails four different challenges which are distributed over three days. Through the participation in each of the four different challenges the teams can achieve a score which will be weighted according to every challenge weight and an overall result is calculated at the end. The main challenge is called "Longrun", its objective is to meet the maximum number of laps on the circuit during 24 continuous hours. The racing strategy in this case is to define the optimal speed in order to maximize the distance travelled for a fixed time and subject to different energy and race restrictions.

1.1.3 American Solar Challenge - ASC

This challenge is a solar car race across the United States. Is held every two years with different routes for every event. Unlike the WSC, the ASC is a rally-style event where the vehicles are timed in a series or predetermined stages, the total race length varies around 3000 kilometres. This way, all the teams stay together during the entire race. The total elapsed time, summing all the stages is the evaluation criteria, therefore, the winner is the vehicle with the shortest time. Accordingly, the race strategy objective is to minimize the sum of all the stage times, subject to the race conditions.

1.1.4 Other races

In addition to the previous competitions, there are other races with specific conditions and restrictions. The “Sasol Solar Challenge” in South Africa and the “Carrera Solar Atacama” in Chile are long distance competitions in the outback of these countries, as the WSC and the ASC, they are carried out in open roads.

On the other hand, Japan leads the on-circuit solar car races with the annual Suzuka solar car race, in the Suzuka International circuit. Although this is also an endurance race, special emphasis is made on the vehicle dynamics in order to control the vehicle and find the most energy efficient path along the circuit (Atmaca [2015]).

1.2 Energy management strategy for land vehicles

The energy management strategy for electric land vehicles has been reported as an optimal control and optimization problem. For Hybrid Electric Vehicles (HEV), the main objective is fuel economy improvement and pollution reduction. Their energy management strategy is based on the power source decision according to the user demand and road conditions (Musardo et al. [2005]). In this case, the control does not include a how-to-drive strategy as it only decides the instantaneous powertrain ratio between the electric motor and the internal combustion engine.

Regarding train operation control, several studies have been reported and disclosed. The principal optimization objective in these cases is to minimize the energy consumption of a train that travels between two points and subject to a defined trip time and some other driving conditions (Vanderbei [2001]). Compared to solar cars, the train energy management includes less uncertainties, mainly due to the absence of the solar energy input and road traffic conditions. The train energy consumption calculation is similar to electric and solar vehicles, especially because the high dependence on the velocity is maintained. Howlett and Pudney (Howlett [1996, 2000], Howlett et al. [2009]) have applied optimal control techniques to mathematically find optimal driving patterns that minimize the energy spent. Chang and Sim [1997] firstly proposed the use of Genetic Algorithms (GA) for optimizing the train coasting segments between two stations with a multiobjective optimization to include the spent energy, the punctuality and the passengers comfort on the objective function. From there, on the last two decades, several applications of GA and other heuristic methods to minimize the train energy consumption on different cases have reported successful results (Han et al. [1999], Lu et al. [2013], Ghaviha et al. [2016]).

1.3 Solar Cars Racing Strategy

The competition strategy of the solar cars raises a set of questions that aim to maximize their performance. Given a specific vehicle, for a defined route, with competition and environmental restrictions and random variables that affect its performance, it must be decided how to operate it in order to optimize its energy performance. Due to the competitive nature, most solar car teams reserve their development and progress. Although information about race strategy of some solar car projects is published, its confidential nature restricts the details and complete descriptions of the recent developments.

Solar car racing strategy can be treated as a control optimization problem where, in the most general case, a velocity pattern for the vehicle must be found in order to minimize the time to complete a defined distance considering race, energy and environmental conditions. The route planning and selection (Hasicic et al. [2017]) are excluded from the race strategy considering that solar car races have a strictly defined path.

Regarding solar cars in general, the most relevant publications are “Speed of Light” (Roche [1997]) and “The Leading Edge” (Tamai [1999]), These two books include some basic information and a general description about racing strategy. On 1998, Shimizu et al. [1998] described the racing strategy of the “Honda Dream” solar car during the 1990, 1993 and 1996 WSC races. They divided the racing strategy on three principal topics: a “Supervision support system”, a “Cruising simulation program” and a “Power/Speed optimizing control algorithm”.

The aim of this work is on the optimization algorithm, including by nature, the simulation program. The supervising support system that is mainly related to telemetry hardware and software is of prime importance for the energy management strategy because a closed-loop control must be implemented due to the different uncertainties of the long races, nevertheless this system is out of the scope of this work.

To find a solution to the optimization problem, two different techniques may be considered: The use of analytic methods based on optimal control theory or the implementation of numerical methods. The analytic solution of this problem has been mainly studied by Peter Pudney and Phil Howlett and disclosed in a series of evolving publications (Howlett et al. [1997], Howlett and Pudney [1998], Pudney and Howlett [2002]). Given specific conditions, different strategies are proposed: speedholding (Howlett et al. [1997]), critical speed strategy (Pudney and Howlett [2002]), constant power for steep inclines or regenerative braking for steep declines (Howlett and Pudney [1998]). According to Pudney and Howlett [2002], taking into account a more realistic model of the battery, the speedholding must be replaced by the critical speed strategy. Other specific situation is discussed when intermittent clouds are present on a level road, in this case high speed under clouds and low speed under the sun (“sun chasing” strategy) is recommended by Shimizu et al. [1998] and Pudney [2000], but the contrary solution is suggested by Daniels and Kumar [1999]. Although these last three conclusions are demonstrated and validated, they differ on initial conditions and vehicle parameter assumptions, resulting on opposite solutions. On the other hand, numerical approaches for solar car racing strategies propose to create a more detailed race simulation model, including complex mathematical definitions and random variables, and then find the optimal velocity of the vehicle using a numerical method. This way, a more case-specific solution is achieved and several recalculations can be made during the race, reaching real-time optimal control in some cases (Guerrero Merino and Duarte-Mermoud [2016]). Dynamic Programming (DP) strategies have been reported by Scheidegger [2006] and Daniels and Kumar [1999], both propose the problem division in long (entire race) and short term (30-minute intervals) strategy. They include the solar radiation prediction as a stochastic variable and take it into account for the long term energy planning. Nevertheless, several assumptions are made to this variable in order to include it on a stochastic DP algorithm. The DP optimization method for the short term is based on a shortest path problem with a time discretization, using the energy consumed on a given time interval as the control function and the travelled distance as the cost function to be maximized on every time step.

A race optimization approach based on optimal control is done by Guerrero Merino and Duarte-Mermoud [2016] with a three scales division. The long term strategy roughly predicts the entire race energy collection and defines a daily consumption, this scale demands a previous estimation of the number of days to reach the finish line and is calculated once per day. The medium term strategy is called daily planning, the race day is divided in 15-minute segments and an optimal energy consumption is defined for the current state and remaining daytime, this stage is recalculated several times during the day. Finally, the short term strategy is called continuous planning, it uses the real-time telemetry data (position, velocity and State Of Charge-SOC) as the initial state to maximize the distance to be travelled according to the energy budget defined on the medium term strategy. Pseudospectral methods are used on this short term strategy to discretize the time variables and reduce the computing time of the control optimization process. The meteorological variables are mentioned as uncertain inputs of the simulation and are approximated based on historical data.

The Boulgakov's thesis (2012) presents a detailed description of the vehicle characterization and mentions the race strategy, simplifies the problem assuming the constant speed during the whole journey but it does not go into details of the optimization method used. In this thesis, special emphasis is made on meteorology, it is mentioned that they take into account a climate prediction, supplied by a meteorology company, with variables such as winds, radiation, precipitation and cloudiness. Finally, they clarify that they only implemented the radiation module due to time restrictions before the race.

De Geus (2007) narrowly described the strategy of the “Nuon Solar Team” of the TU Delft University and sponsored by N.V. Nuon Energy from the Netherlands. This team has won seven times of nine total participations in the WSC and is always referenced by the other competitors. The publication mentions, without going into detail, that Nuon has used DP and divided the strategy into overlapping optimization subproblems. A long-term optimization as well as Scheidegger [2006] and the medium term for each race day. It is also mentioned that they used genetic algorithms as an optimization method. To include the climate, they used a database of more than 20 weather stations distributed along the route. The update of this database in the race is done through satellite internet.

Besides Nuon, other evolutionary algorithms are reported for solar car strategies. The Solar Car Team of University of Michigan reports the use of genetic programming to solve their strategy problem on a weather forecasting disclosure (Shao et al. [2016]).

On 2013, Yesil et al. [2013] proposed an heuristic optimization using the Big Bang-Big Crunch (BB-BC) method (Erol and Eksin [2006])) for the 2013 WSC, they do not compare the results with other methods and experimental validation is missing. Nevertheless they reported a satisfactory outcome with their implementation. Following this disclosure, Onol et al. [2017] developed a sensitivity analysis of different vehicle variables based on the same BB-BC optimization. The influence on the total race time induced by 15% variations on the vehicle mass and aerodynamic coefficient is simulated and quantified. Regarding solar irradiation variations, a new simulation with induced cloudy conditions is executed, for this case, the battery is drained before the end of the race forcing solar charging stops. The optimization method efficiency and convergence is not reported.

According to the aforementioned descriptions, several approaches have been made from different points of view to the solar cars racing strategy. There are methods based on simplifications to arrive at optimization problems with mathematical solution. Nevertheless, in most of the real cases, the solar car racing strategy includes so many variables to take into account that mathematical solutions move away from real cases by their level of idealization.

On the other hand, optimization models are proposed based on numerical methods. In most of the cases, these methods do not have a mathematical approach that guarantees that a global optimum will be reached, but they allow to solve more complex problems and include more variables in the model. The implementation of evolutionary algorithms to optimize the race strategy has been reported by different projects. These optimization methods become an attractive solution due to their ability to include complex models, variations and nonlinear functions to the race simulation while the optimization algorithm will still find a competitive solution. Besides, the growing computational capacity, including parallel computing, opens field for the efficient application of these methods.

1.4 Meteorological variables

Wind speed and solar radiation directly affect the performance of the solar vehicle and their accurate prediction is a decisive factor for the race strategy success. For solar cars applications, these meteorological variables must be predicted on the short-term future (1 to 6 days) and for the different locations that the vehicle may reach. Therefore, for example the WSC strategy demands a meteorological prediction for 6 days over the 3022 kilometres road.

1.4.1 Wind speed

For the energy consumption model, the wind velocity vector with respect to the vehicle advance direction might be estimated. A crosswind affects the vehicle aerodynamic drag and strongly influences its stability (Volpe et al. [2014]) while the head and tailwinds also bias the aerodynamic drag and therefore the energy consumption. The inclusion of wind speed variables has not been reported in detail nor there is evidence of its successful implementation in solar car racing strategies. As stated by Guerrero Merino [2013], historic data is recommended to statistically estimate a wind velocity average speed and direction for the race days over certain locations. Onol et al. [2017] on the other hand, highlight the unpredictability of this variable and recommend real time data processing from weather stations to reduce the uncertainty.

Concerning wind energy production applications, several models using time series or numerical weather prediction are reported with satisfactory results for a short term window (Giebel et al. [2011]). Time series are commonly used for short term predictions (up to 6 hours ahead) while numerical models may give insights up to 48 hours. Compared to wind turbines, the solar car demands an estimation for a moving target and a greatly lower height going from 0.4 to 10 meters above the ground. Therefore, the wind velocity may be considered as the most stochastic variable, its prediction requires small scale atmospheric models and big uncertainty for a time horizon of more than 8 hours is reported.

1.4.2 Solar radiation

The solar irradiance is defined as the power density received by a surface by means of the solar radiation, in Watts per square meters (W/m^2). This value, calculated as the sum of direct and diffuse components, is called Global Horizontal Irradiance (GHI). Then, the electrical power produced by a solar panel may be estimated by multiplying the GHI by the collector effective area and its global efficiency. In this way, predicting the energy produced by the solar car involves a forecasting of the GHI for the different positions and times of the vehicle in race.

On this state of the art, it should be clarified that the term “estimation” is referred to the calculation of the instantaneous or average variable of interest in the present or past time, while “prediction” refers to the forecast of future values.

Historical data averages and regression models are commonly used for predicting the solar irradiance on solar car strategies. Onol et al. [2017] use the GHI historical average on five locations over the route to predict the race days.

Shao et al. [2016] predict an hourly average GHI for the University of Michigan Solar Car Team using machine learning and big geospatial data. More precisely, a quantile regression structure is implemented in order to define probability confidence ranges for the irradiance, resulting on different quantiles predictions for varied scenarios. The GHI forecast is achieved using a combination of two meteorological models: The Global Forecast

System model (GFS) developed by the National Oceanic and Atmospheric Administration (NOAA) and the European Center for Medium-Range Weather Forecast (ECMWF) model. These two models are cleverly combined through a specific-case machine learning approach, where the system is trained using measured data from March 2015 to the first two weeks of May 2015 and validated with the last two week of May 2015. As expected, the P50 quantile obtained from this implementation shows better results than the independent GFS and ECMFW models.

Additionally to its applicability in solar car races, the precise estimation and prediction of GHI over large areas has gained significant importance due to the solar photovoltaic energy growth. Meteorological stations are able to measure local irradiance with high precision and frequency but they are spatially fixed and their distribution is not enough to generate valid interpolations over large areas between them.

For any location, on a given date and time with a complete clear sky (no clouds), the GHI can be calculated and estimated with a Root Mean Square Error (RMSE) under 6% (Gueymard [1993]) using a clear sky model. The clear sky models found in literature differ between them on the complexity of the atmospheric models included, passing from a simple air mass calculation (Leckner [1978]) to more complete atmospheric transmittance considerations based on the different aerosol particles present (REST2 - Gueymard [2008]).

Regarding the clouds inclusion, the clouds effect on the GHI is commonly represented using the Clear Sky Index (K_c), this index is defined as the ratio between the measured and the clear sky GHIs (See Equation 1.1).

$$K_c = \frac{GHI}{GHI_{clr}} \tag{1.1}$$

Where GHI represents the observed and GHI_{clr} the clear sky estimated global horizontal irradiances. In this sense, solving the Equation 1.1 for GHI, the solar irradiance estimation is defined as the combination of two factors: the clear sky irradiance that can be precisely determined and the clear sky index that mainly depends on the clouds and introduces uncertainty to the estimation.

High quality satellite images are continuously available for the entire world and include implicit information about the K_c over large areas, allowing the detection of clouds, rain, among other influential atmospheric conditions. Image processing techniques have been implemented in order to identify and estimate these meteorological conditions, also the application of machine learning methods based on satellite images has been reported with satisfactory results (Pelland et al. [2013]).

According to Kleissl [2013], an estimation for hourly solar radiations using semi-empirical satellite models can achieve a normalized Root Mean Squared Error (nRMSE, see Equation 3.5) in the range of 7%-20% for arid and semiarid areas. In tropical, more cloudy or mountain regions, this expected nRMSE may increase to the range of 15%-35%.

Several projects have reported the GHI estimation and prediction using satellite images. In 1986 Cano et al. [1986] introduced a novel method (called HELIOSAT) based on the use of satellite images in order to obtain a reference map of the albedo (I.e. reflectance) of each coordinate of a scene, afterwards, the images are compared to the reference albedo map, and a K_c index is calculated. Rigollier et al. [2004] proposed several improvements to the HELIOSAT by introducing more physical and optical variables to the calculation, instead of sensor scale variables, this method is called HELIOSAT-2. Upon the approach presented by Cano et al. [1986], Boulifa et al. [2015] constructed a method based on the intensity level of each pixel within the satellite image, using Meteosat Visible High Resolution (HRV) images, and calculated a cloud index from the different levels of intensity in the image, although the HELIOSAT and HELIOSAT-2 methods are more complex and robust, this method presents the advantage of directly obtaining an indicator of the cloud scene from the information contained in the image without further processing and calculations.

From satellite images and resorting to machine learning, Artificial Neural Networks (ANN) have been satisfactory implemented in this field (Yadav and Chandel [2014], Voyant et al. [2017]). These approaches are regression models based on statistical techniques that might be trained using a large set of known dependent variables (or outputs) and their corresponding independent variables (or inputs), this way a generalization is expected to predict other outputs given new inputs. Therefore, a data procurement and preprocessing is demanded and is commonly the most time-expending task of these procedures.

Methods using neural networks to estimate the solar irradiance with satellite images have been mainly focused on Multilayer Perceptrons (MP) architectures (Linares-Rodriguez et al. [2013], Marquez et al. [2013], Quesada-Ruiz et al. [2015]). Zarzalejo et al. [2005] firstly proposed the use of ANN and satellite images to estimate the hourly solar radiation over Spain, their network input is the cloud index derived from satellite image processing and their outcome is called atmospheric transparency index which is equivalent to the K_c index explained before. Linares-Rodriguez et al. [2013] proposed an ANN based on MP to estimate the daily solar radiation over Andalusia (Spain), satellite images on 11 different wavelengths taken every 15 minutes and a clear sky GHI are used as input. A RMSE of 6.74% on a daily basis is achieved, outperforming previous methods. More recently, Quesada-Ruiz et al. [2015] proposed an hourly GHI estimation with an ANN improvement with respect to previous works, an ensemble of different ANNs is proposed in order to first classify the image scene in three groups according to the sky conditions and then send it to the corresponding ANN (overcast, intermediate or clear sky). A nRMSE of 13.5% for the hourly GHI estimation is reported with the combination of these two MP neural networks, one that classifies the scenes according to the cloud index and other that calculates the GHI for any cloud condition. The ANN input parameters are 11 channels of the satellite images (including visible and infrared ranges) and the GHI_{clr}. All the disclosures discussed above, used data for training and validation from the Meteosat geostationary satellite which covers the European, African and West Asia regions.

Marquez et al. [2013] combined the GHI estimation using ANN with a short term (up to 120 min) prediction for the 30-minutes average GHI. The cloud indexation and velocity are obtained from the time series of previous images and included in the ANN, the RMSE of the GHI prediction ranges from $50Wm^{-2}$ for 30 minutes to $80Wm^{-2}$ for a 120 minutes forecast.

According to the project necessities, satellite images are proven to include the information to accurately estimate and predict the GHI in the short term future. Although most validations are made over European regions, the approximations presented above may be the start point to a valid GHI estimation for solar car races.

Chapter 2

Solar car energy management: model and heuristic optimization

The content of this chapter has been published in Betancur et al. [2017c].

Solar cars are known for their energy efficiency, and different races are designed to measure their performance under certain conditions. For these races, in addition to an efficient vehicle, a competition strategy is required to define the optimal speed, with the objective of finishing the race in the shortest possible time using the energy available. Two heuristic optimization methods are implemented to solve this problem, a convergence and performance comparison of both methods is presented. A computational model of the race is developed, including energy input, consumption and storage systems. Based on this model, the different optimization methods are tested on the World Solar Challenge 2015 race strategy under two different environmental conditions. A suitable method for solar car racing strategy is developed with the vehicle specifications taken as an independent input to permit the simulation of different solar or electric vehicles.

2.1 Introduction

Solar car races are well-known as universities and college competitions with the aim of promoting alternative energies and energy efficiency. Nevertheless, major engineering developments are required to have a competitive vehicle and several developments that have emerged in these races are now applied in different industrial sectors. High efficiency electric motors and drivers (Yamazakii et al. [2017]), low consumption tires, solar panel Maximum Power Point Trackers (MPPTs), solar panel encapsulations and telemetry systems are some of the technological products raised on racing solar cars Connors [2007].

The WSC is one of the most popular solar vehicle races where recognized universities and industries from all over the world join forces to compete every two years. The main objective is to cross Australia from Darwin to Adelaide (3022 km) using only solar energy.

The success on this challenge demands both an efficient vehicle and an adequate control strategy during the entire race (World Solar Challenge [2018]).

The vehicle must be designed, built and raced with the purpose of being energy efficient. The main features of the car are based on two properties: reliable and autonomous. For the autonomy, the car should capture as much as possible energy from the sun and spend the lowest possible energy when traveling. The design and manufacture processes take into account: reliability, safety, solar panel efficiency, aerodynamics, weight reduction, among other important considerations (see Minak et al. [2017], Tamura [2016], Paterson et al. [2016], Betancur et al. [2017b], Vinnichenko et al. [2014]).

With the vehicle conceived, the final step is to define the race strategy in order to obtain the best performance and take advantage of its capabilities. The narrow gap between the energy input from the solar panel and the consumption of the motor creates the necessity of optimizing the driver decisions seeking a good energy management. The race plan must define the speed on the entire path, taking into account the vehicle properties, the road characteristics, the weather conditions, and all the factors that can affect the vehicle or the race development. The solar car racing strategy problem has been narrowly disclosed academically due to the competitive nature of cars racing. Since the early 90's, less than 10 studies about this topic have been formally published. On the contrary, train optimal control has been widely studied and disclosed for decades. Although several differences are remarkable, the energy efficiency operation is the main objective of both applications and different approaches can be applied on solar cars. Following the state of the art reported in Sections 1.2 and 1.3, a heuristic optimization approach is proposed and the optimization results are compared with previous approaches.

In this work, the racing strategy of the EPM-EAFIT solar car for WSC 2015 is presented. Section 2.2 describes the race model in order to simulate the vehicle performance for a given conditions. Once the race model is complete, an optimization process is linked to this model and the best driving parameters are found in order to minimize the objective function, i.e. racing time (See Section 2.3). Three different optimization methods are tested and results are exposed on Section 2.4.

2.2 The Race Model

The first step for optimizing a solar car performance is to model the vehicle behavior on the race. With this race model, the consequences of different strategy inputs on the race performance are obtained.

For a solar car simulation, three main models should be coupled together: battery, motion equations (energy consumption) and solar panel (energy input). The environmental conditions affect the energy input via radiation and temperature and the energy output mainly because of the wind that influences the drag force. Then, they are considered into an independent module of the race model. Figure 2.1 illustrates the interactions between modules on the model.

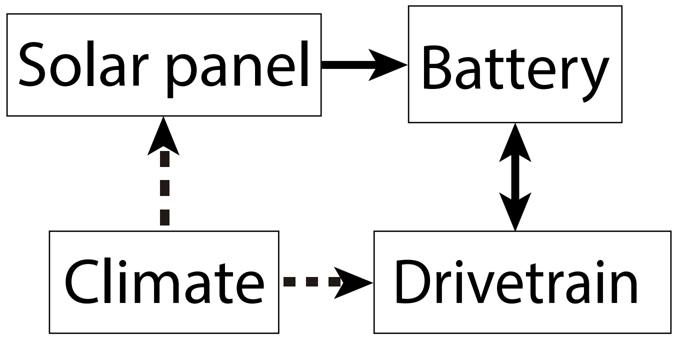

Figure 2.1: The car model overview of the four main coupled models simulating the solar vehicle performance on a given race.

In order to accurately estimate the vehicle performance in the race, the model should include all the car characteristics such as weight, roll coefficient, aerodynamic properties among others. Also external information like road slope, sun position, sun irradiation, wind and others should be considered. This model must be tuned up and validated with experimental tests of the vehicle to expect valid results.

One of the main inputs of the race model is the velocity set point for the whole race. This is a user (driver) input that affects the outcome on the competition. The velocity set point is a curve that indicates the speed of the car during the race. According to the practical limitations in the race, this velocity is defined to be an integer number in kilometers per hour (km/h) and bounded by the speed limits of the road. Moreover, although the velocity set point can change every instant, it is practical to keep it constant for certain periods of time, generating this way a vector that contains the velocity set point for defined segments of the race. Then, the size of this velocity vector is the same number of divisions of the race made for the optimization process.

2.2.1 Drivetrain

The energy consumption of the vehicle is simulated using the drivetrain model. The main forces that directly oppose the vehicle movement are: aerodynamic drag, tyre rolling resistance and gravity component due to the road slope. The instantaneous power needed on the drive wheels can be calculated as defined in Equation (2.1) where P_m stands for the instantaneous motor power, v for the instantaneous velocity, m for the vehicle mass, a for the acceleration, C_dA is the vehicle drag area coefficient, ρ the air density, v_w the wind velocity component on the vehicle forward direction, C_{rr} the tyre roll coefficient, g the gravity acceleration and θ the road slope.

$$P_i = v\left(ma + \frac{1}{2}C_dA\rho(v - v_w)^2 + C_{rr}mg + mg\sin\theta\right) \tag{2.1}$$

For road sections with constant slope and velocity, the wheel power remains constant and the consumed energy (E_i) can be calculated according to the time (t_i) on the respective section and the drivetrain efficiency under these conditions (η_m). Equation (2.2) defines the consumed energy estimation for constant speed sections.

$$E_i = \frac{P_m t_i}{\eta_m} \tag{2.2}$$

In the case of Csiro motors, the instantaneous drivetrain efficiency is estimated according to the study reported on Al Zaher [2010].

2.2.2 Solar Panel

The photovoltaic solar panel energy generation is simulated taking into account the sun elevation angle (ϕ), the estimated solar irradiance at ground level (I_i) (See Section 2.2.4), the panel and electronic circuit efficiency (η_s) and the panel effective area (A_s) that considers the instantaneous canopy shadows over the cells. The electric power produced by the solar panel (P_s) is calculated as defined on Equation (2.3).

$$P_s = I_i A_s \eta_s \sin(\phi) \tag{2.3}$$

The solar panel efficiency is experimentally determined taking into account the forced convection cooling of the cells due to the vehicle movement as reported in Vinnichenko et al. [2014].

2.2.3 Battery

A battery model is developed according to the specific cells datasheets and duty cycle experiments. Based on the charge and discharge data integration, the input and output energy are calculated and the battery overall efficiency (η_b) is estimated according to Equation (2.4) where E_{out} and E_{in} represent the total energy obtained from the discharge and charge test cycles. The energy stored in the battery (E_b) is defined by Equation (2.5) where P_s and P_m are the instantaneous solar panel power and drivetrain power respectively, the charge and discharge efficiencies are assumed both equal to $\sqrt{\eta_b}$.

$$\eta_b = \frac{E_{\text{out}}}{E_{\text{in}}} \tag{2.4}$$

$$\frac{dE_b}{dt} = \begin{cases} \sqrt{\eta_b}(P_s - P_m), & \text{if } (P_s - P_m) > 0 \\ \frac{1}{\sqrt{\eta_b}}(P_s - P_m), & \text{otherwise} \end{cases} \tag{2.5}$$

2.2.4 Climate

The more relevant climate factors that affect the vehicle simulation are the solar irradiance (See Equation (2.3)) and the wind velocity vector (See Equation (2.1)). The stochasticity of these two variables is removed in order to guarantee repeatability of the optimization process. Nevertheless, a clever estimation of both parameters is included in the simulation.

The solar irradiance (I_i) is calculated according to the air mass factor and the Lambert's law (also known as Beer–Bouguer–Lambert's Law) to define the atmospheric transmittance (Iqbal [2012], Leckner [1978]). Cloudless sky is assumed and the model is validated experimentally. Equation (2.6) defines the radiation estimation, I_0 represents the extraterrestrial solar radiation, τ^a the total atmospheric extinction or attenuation coefficient and AM the air mass factor (defined on Equation (2.7)).

$$I_i = I_0 \mathrm{e}^{-\tau^a AM} \tag{2.6}$$

$$AM = \frac{1}{\sin(\phi)} \tag{2.7}$$

On the other hand, the wind velocity vector is estimated and included according to the monthly averages reported online by the Australian Government Bureau of Meteorology (Australian Government, Bureau of Meteorology [2017]).

2.3 Optimization Process

A heuristic optimization approach, as described in Section 1.3, is selected for defining the race strategy. The main purpose is to find the best velocity in order to minimize the solar car racing time. To have an accurate race model, the optimization step is implemented as depicted in Figure 2.2. Different velocity vectors are produced by the optimization algorithm and evaluated in the race model.

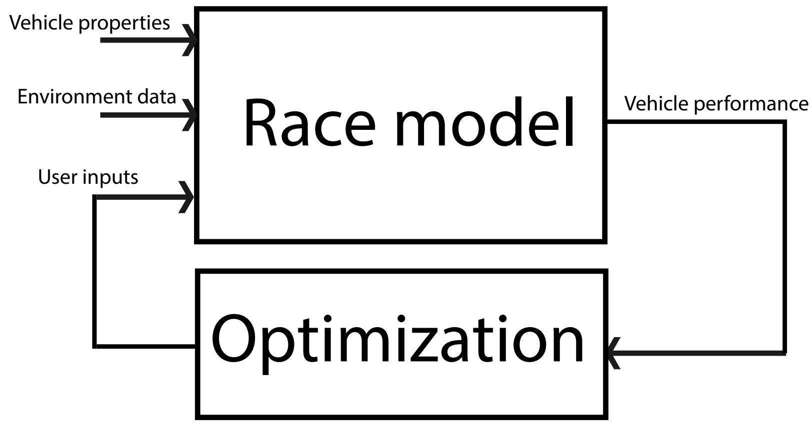

Figure 2.2: The purpose of the optimization process is to find the optimal user input for the race model in order to minimize the objective function

The number of race divisions for the velocity vector defines the search space size. When the velocity is assumed constant all over the race, the optimization variable is a 1-dimensional vector and a global optimum solution can be found with an exhaustive search. On the other hand, with large velocity vectors, a larger search space is created and clever optimization techniques are needed to find a near-optimal solution. Then, different optimization techniques are used depending on the optimization variable size.

2.3.1 Exhaustive Search

To be sure of finding a global optimum, the first optimization method is the well-known Exhaustive Search (ES), also named brute-force search. The purpose is to test all the possible solutions and choose the best one. In the case of a 1D velocity vector, it is possible to test all the integer numbers between velocity bounds and pick the best, if the optimization variable is greatly larger it results as non-viable to test all the possible combinations.

2.3.2 Genetic Algorithms

As proposed by John Holland (1975), Genetic Algorithms (GA) is an evolutionary method based on natural populations and genetic studies to mimic a biological evolution process. With a combination between the natural selection process in which “most fit individuals survive” and random events such as coupling and mutating, an evolution towards an optimal solution is guaranteed. Since the 1970s, new implementations, variations and improvements have been developed showing the large capabilities of this method. For the solar car race strategy problem, a GA is implemented following recommendations given by Sastry et al. (2014).

2.3.3 Big Bang-Big Crunch

An alternative evolutionary optimization method already implemented on solar car strategy by Yesil et al. (2013) is called Big Bang-Big Crunch (BB-BC). It was first developed by Erol and Eksin (2006) reporting an efficiency improvement with respect to a general GA method. The general aim of this method is to iteratively generate random individuals around a center of mass (big bang) and recalculate the center of mass according to the weighted average fitness of the population (big crunch). On every iteration, the radius for new individuals generation is reduced in order to progressively diminish the search space. Equation (2.8) defines the way to calculate this value, where $\bar{x}^c$ is the center of mass, n is the population size, $\bar{x}_i$ is an individual of the population and f_i its fitness value.

$$\bar{x}^c = \frac{\sum_{i=1}^{n} \frac{1}{f_i}\bar{x}_i}{\sum_{i=1}^{n} \frac{1}{f_i}} \tag{2.8}$$

An implementation of the standard BB-BC algorithm is also made and tested for this project.

2.3.4 Algorithm Hybridization

To improve the optimization performance, a combination of different methods is proposed. In this case, a Local Search (LS) step (Gonzalez [2007]) is included after the GA and BB-BC processes as reported on Ishibuchi and Murata [1996]. One-directional variations are made iteratively to the solution given by the evolutionary algorithm, more precisely the velocity of every section of the race is modified ($\pm 1km/h$) and this solution is evaluated. This has the purpose of evaluating the candidate solutions in the vicinity of the evolutionary algorithm result, if the objective function result is improved, this new solution is saved and the process is iteratively repeated.

2.4 Results

To solve the problem of finding an optimal speed for the EPM-EAFIT Solar Car, for the 2015 WSC, different approaches are implemented and compared. Two environmental cases are proposed: a fully clear sky race (Clear sky case) and a race with one cloudy day that diminishes the entire day irradiance to a 60% of the clear sky one (Cloudy day case). Figure 2.3 illustrates the solar irradiance estimation for both cases.

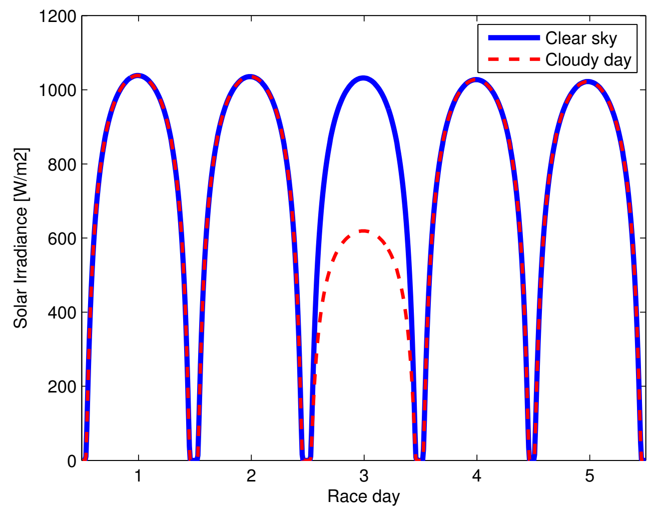

Figure 2.3: Solar irradiance for the first 5 days of the race. In the case of Cloudy day, the irradiance of day 3 is reduced to the 60% of the clear sky estimation.

Regarding the optimization method, five main approaches are analyzed for the two environmental cases:

- Constant speed during all race (1D optimization variable) with exhaustive search optimization.
- Race length divided into halves, two different speeds (2D) and exhaustive search optimization.
- Race length divided in three parts, three different speeds (3D) and exhaustive search optimization.
- Race divided in 10 segments (10D optimization variable) according to mandatory 30 min control stops defined by the race and GA evolutionary method optimization.
- Race divided in 10 segments (10D optimization variable) according to mandatory 30 min control stops defined by the race and BB-BC evolutionary method optimization.

The ES is not implemented with more than 3D vectors due to the large number of possible combinations, in these cases the time required to finish the calculation is considerable. The GA and BB-BC methods are both implemented with 10D vectors and a constant population of 720 candidates, this resulted from experimental grid search of different population sizes. The initial population is created with a random number generator between the minimum velocity and the road speed limit with a uniform distribution.

Every GA iteration involves:

1. Evaluation of the fitness function (race simulation) for every candidate. The best individual is saved.

2. Selection of the most fit individuals. The best half of the population is saved for crossover.

3. Crossover. Random pairs of individuals (parents) are selected from the saved population and four new candidates (sons) are obtained with a linear combination of every pair.

4. Random mutations are included on the population. An aleatory number from an uniform distribution between -10 and 10 km/h is added to a 10% of the new population.

These steps are repeated until the maximum number of iterations is reached. Also, an early convergence criteria is defined to stop the iterations.

For the BB-BC implementation, the steps 2 and 3 from GA are replaced by the calculation of the center of mass and random generation of new individuals around it, as it is explained on Section 2.3.3. The other steps are performed as explained for GA. For both methods a limit of 50 iterations is defined. The hybridization proposed on Section 2.3.4 is evaluated with the GA+LS and BB-BC+LS algorithms.

The obtained results for a given specific solar car properties, road and the Clear sky weather conditions are shown on Table 2.1, the results for the same vehicle properties and road but Cloudy day weather conditions are shown on Table 2.2. The listed results are the average of 15 runs of every algorithm. The typical convergence graph for the two different weather cases is presented on Figure 2.4. Both the race simulation and the optimization method are programmed in C++ using Microsoft Visual C++ editor and compiler under Windows operative system, then executed serially (not on parallel) on a laptop with Intel Core i7 @ 2.3GHz processor.

Table 2.1: Optimization methods results for Clear sky race.

Optimization Method	**Optimization Vector Size**	**Obj. Function Value [h]**	**Computing Time [s]**	**Total Race Simulations**
Exhaustive search (1)	1	38.189	0.28	61
Exhaustive search (2)	2	38.189	14.85	3721
Exhaustive search (3)	3	38.077	926.46	226981
Genetic Algorithms	10	38.104	137.29	36000
GA+LS	10	38.074	145.16	36810
BigBang-BigCrunch	10	38.174	141.34	36000
BB-BC+LS	10	38.093	150.65	38430

Table 2.2: Optimization methods results for Cloudy day race.

Optimization Method	Optimization Vector Size	Obj. Function Value [h]	Computing Time [s]	Total Race Simulations
Exhaustive search (1)	1	40.176	0.39	61
Exhaustive search (2)	2	39.929	21.13	3721
Exhaustive search (3)	3	39.792	1284.1	226981
Genetic Algorithms	10	39.818	116.44	28800
GA+LS	10	39.788	120.89	29610
BigBang-BigCrunch	10	39.878	197.96	36000
BB-BC+LS	10	39.796	209.01	38025

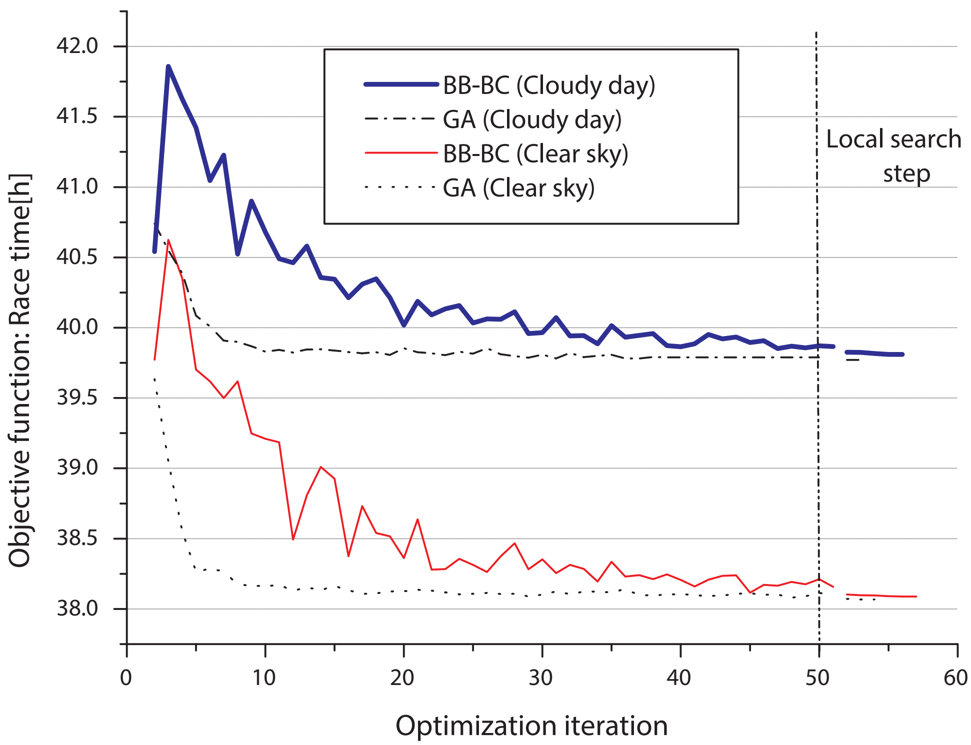

Figure 2.4: Race optimization using Big Bang-Big Crunch and Genetic Algorithms methods for Clear sky and Cloudy day cases. After 50 iterations, the local search step is included for both methods.

2.5 Case Study

The optimal speed found is only valid for the vehicle properties defined on the race model input. This optimal speed produces a curve that indicates the optimal State Of Charge (SOC) of the battery during the entire race. Figure 2.5 illustrates the SOC behavior according to the best solution found using GA+LS and considering the two environmental cases. The optimal velocity vectors are also depicted.

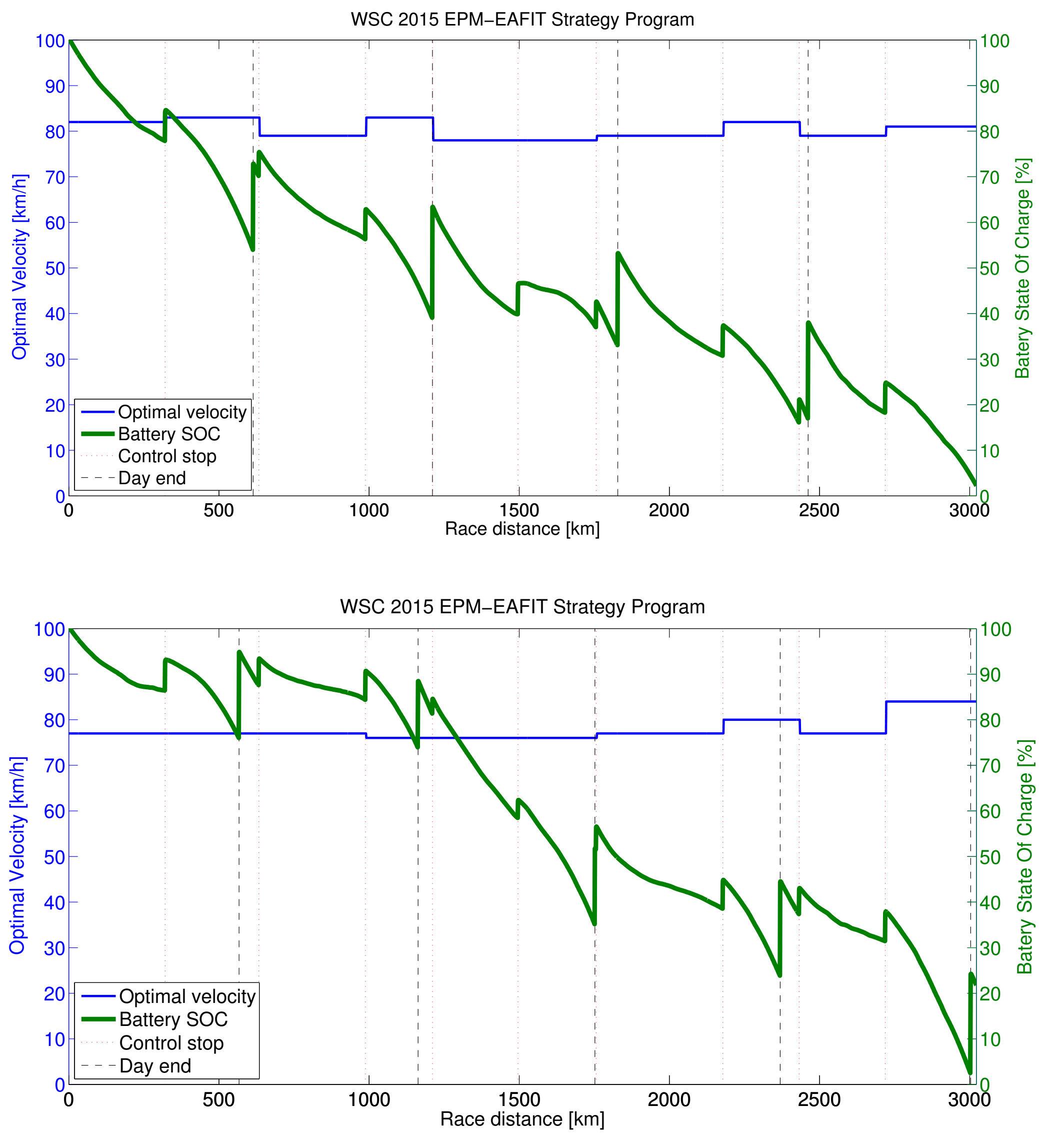

Figure 2.5: Optimal State of charge of the battery and velocity vector for different environmental conditions: Clear sky conditions (Top) and Cloudy day conditions (Bottom) The control stops (dotted lines) indicate 30 min mandatory stops, the discontinuous lines indicate the km where the night is spent.

2.6 Conclusions

The solar car racing strategy planning is the activity to define the best user inputs in order to optimize the energy management and, therefore, minimize an objective function. In this case, the objective function was the time to arrive to the finish line, namely race time, subject to limited energy and other vehicle, road and environmental constraints.

The selected optimization algorithm depended on the size of the search space and the time required to run one single simulation. In this case, one race simulation needed between 4 and 6 milliseconds (ms) of computing time. Then, it was possible to estimate the time needed to execute a defined number of simulations. When an exhaustive search was not practical due to the expensive running time, an evolutionary method was recommended.

In the two cases of study, the GA showed faster convergence and better result than the BB-BC, moreover a monotonic decreasing tendency over the iterations was observed in the graph. Both evolutionary tested methods did not find a global optimum solution, this was verified with the LS step added after, given the small improvements obtained with this hybridization in all the cases.

Enlarging the search space by increasing the number of race divisions produced better solutions than 1, 2 or 3D optimization variables, taking into account that in the case of 10D velocity vectors finding the global optimum solution was not guaranteed with the methods used. No difference was obtained with the change of 1D to 2D, but a 3% (equivalent to 7 min on race) reduction was reached with the 10D vector. The ES method with 3D vectors remarkably exceeded the total race simulations executed (with respect to the other test cases) and, therefore, the total computing time.

The optimal velocity found, was the one that makes the battery SOC end near empty. A 30 min recharging stop was considered if the battery is drained before the finish line but this was evaded in the optimal strategies found. Although a non constant velocity was proved to be better, the 10 optimal velocities for the race kept between 78 and 83 km/h on the Clear sky case and between 75 and 84 km/h on the Cloudy day one. In practical terms if the speed control of the car is manual, this can lead to the same speed all the race.

The 40% solar irradiance reduction on a complete day represented an increase in the race time of almost 2 h, going from a racing time of 38.068 to 39.771 h according to the GA+LS optimization results. The consequences of different environmental cases can also be estimated using this process.

The time efficiency of this optimization method makes it a feasible option to recalculate the strategy during the race after deviations from the predicted behavior or climate prediction changes, a new optimal strategy is obtained in less than 3 min of computing time. This method can be applied to other objective functions and any type of electric vehicle with a given characterization. Other interests can maximize the distance with limited energy or limited time, minimize the external energy used on a given path or optimize the recharging times for a given route.

Chapter 3

Solar resource estimation

A new method based on Convolutional Neural Networks (CNN) for the estimation of the ground solar irradiance is proposed and tested on the continent of Australia. The 3 visible bands from the Himawari-8 geostationary satellite images together with the clear sky irradiance estimation are used as input. The inclusion of a set of contiguous pixels on the input data to improve the estimation is validated. A comparison with Multilayer Perceptron (MP) neural networks and image processing techniques based on pixel intensities is performed. Regarding the estimation accuracy, the CNN and MP neural networks achieved similar results and both outperformed the image processing on this task.

3.1 Introduction

Since the last two decades, the solar energy installed capacity has shown an exponential growth. To the date, the photovoltaic panels cost is still declining resulting on more economically viable solar energy projects. The main advantage of solar energy is the global homogeneity distribution of solar radiation, in comparison with other renewable energy sources such as wind, hydraulic or tidal.

Although the long term statistics may define valid annual or monthly solar radiation cumulatives, the short term prediction and real-time estimation still includes uncertainties mainly produced by the stochastic weather conditions.

These variations affect the solar energy production inducing high fluctuations on the energy grid that may be controlled by the operators or cushioned according to the grid stability. Accordingly, active control services are needed to guarantee the integration of these variable energy sources on the grid.

The precise estimation of Global Horizontal solar Irradiance (GHI), defined as the sum of direct and diffuse irradiances, over large areas has gained significant importance due to the solar photovoltaic energy growth. Meteorological stations are able to measure local irradiance with high precision and frequency but they are spatially fixed and their distribution is not enough to generate valid interpolations over large areas between them.

In this chapter, a comparison between the GHI estimation from image processing techniques and machine learning methods, specifically several variants of artificial neural networks, is executed and compared to the state of the art references mentioned in Section 1.4.2. For training and validation, GHI measurements are obtained from 7 meteorological stations distributed over the Australian territory and the visible range satellite images are obtained from the HIMAWARI-8 geostationary satellite operated by the Japan Meteorological Agency (See Japan Meteorological Agency [2017]).

Convolutional Neural Networks (CNN), are a variation of MP that include a series of convolutional layers. This way, machine learned filters are automatically applied to the input data to obtain better results. In different applications of image related tasks, CNN architectures have proved to excel MP (LeCun et al. [2015]). CNNs have been used to detect and classify objects within images (Krizhevsky et al. [2012]), to colorize black and white images (Zhang et al. [2016]) among other image and non image related tasks. In the medical field CNNs have also been used to detect brain tumors using MR images(Havaei et al. [2017]), and to classify skin cancer(Esteva et al. [2017]).

To the best of the authors knowledge, the use of CNN is not reported on GHI estimations. The state of the art approaches using ANN and satellite images (over several channels) to estimate the GHI only include the target pixel as input data. However other authors use the neighbor pixels (Mefti et al. [2008]), but they do not use machine learning techniques. Therefore, this chapter describes the implementation of a CNN architecture on this area and compares its performance and accuracy with MP neural networks and image processing techniques, the relevance of including the neighbor pixels is also studied.

This chapter is structured as follows. In the next section, a description of the satellite images and observed data used as input, training and validation is presented. In Section 3.3, The methodology for the different estimations of GHI is explained. The results of the different estimations are presented in Section 3.4. Finally, the results discussion and conclusions are made in Section 3.5.

3.2 Data

Two main data types are used, on the one hand GHI observations on different locations in the Australian continent; on the other hand, their corresponding satellite image.

Measurements of GHI are obtained from the Bureau of Meteorology of Australia (Australian Government, Bureau of Meteorology [2017]) at seven different locations as it is shown in Figure 3.1. The dates range from August 2015 to December 2015 at 10 minutes intervals.

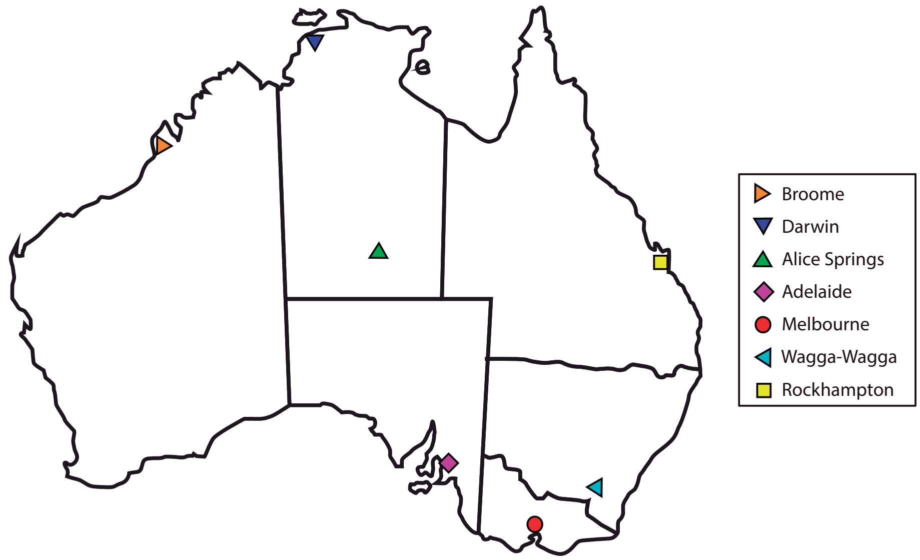

Figure 3.1: Observed GHI data locations on the Australian continent

Satellite images taken by the Himawari-8 geostationary satellite are obtained from the National Institute of Information and Communications Technology (NICT). The first three bands are used, corresponding to 0.47, 0.51 and 0.64 μm wavelengths, which coincide with the visible light. The spatial resolution of these images is 1km per pixel. The images also span from August 2015 to December 2015, taken at 10 minutes intervals. An example of an image is shown in Figure 3.2.

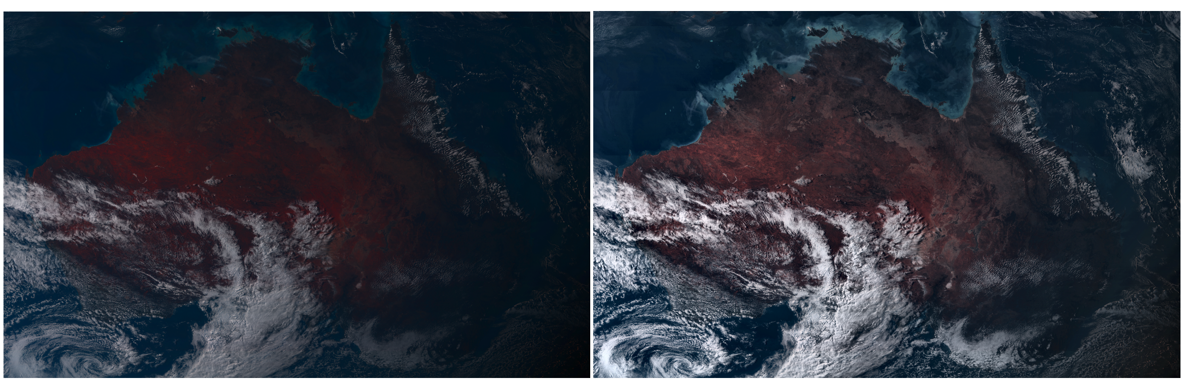

Figure 3.2: Original (right) and equalized (left) satellite images from Himawari-8 visible bands.

The satellite images are equalized, by converting them to the HSV color space, the equalization process is applied over the V (Value) channel, and then converted back to the RGB color space. An example of an equalized image is shown in Figure 3.2. Crops for each station are taken from the satellites images centered at each meteorological station corresponding pixel, the pixel location is calculated from the geographical coordinates following the Himawari-8 data specification Japan Meteorological Agency [2017]. A total crop size of 15x15 pixels is obtained by spanning 7 pixels in each direction (See Figure 3.3). The total data resulted in 79004 observations: 65249 used for training and validation, and 13755 for testing.

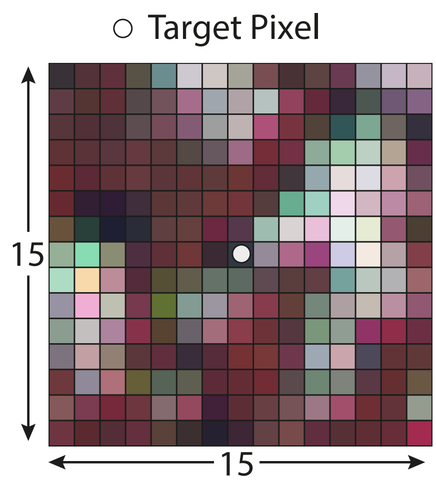

Figure 3.3: 15 pixel image crop example. The center pixel corresponds to the location where the GHI estimation is desired. For the case of Himawari-8 images, the pixel resolution is 1km.

An additional input for the GHI estimation is the clear sky irradiance (GHI_{clr}). This variable is calculated using the ESRA clear sky model (Rigollier et al. [2000]) following Engerer and Mills [2015] conclusions for the Australian continent. The Linke turbidity factor is defined as $TL = 3.323809$, obtained as the Australian yearly average from the data provided by SoDa (Wald et al. [2002]) and assumed constant in time and space over the entire continent.

3.3 Methodology

In order to estimate the GHI from the satellite images for the Australian continent, two principal approaches are proposed. An image processing process based on the pixel intensity to determine the clear sky index (K_c) and a machine learning technique trained with a portion of the data, validated with other portion and finally tested with the same data as the other methods. The two methodologies are explained below.

3.3.1 Image processing

The satellite images include implicit information about the K_c index for every pixel. The presence of visible clouds is the main responsible of the variation of this coefficient. Therefore, this process considers a cloud identification followed by the quantification of their intensity in the pixels of interest.

The cloud identification is carried out using a segmentation technique proposed by Otsu [1979]. The intensity levels of the image pixels, which range from 0 to 255, are divided into two classes, corresponding to pixels with or without clouds. An optimal threshold level is found based on the entropy of the image, for which every pixel over it is considered as value 255 and every pixel under the threshold level is considered as value 0. Building up from this method, a 3-channel segmentation is executed, where the remaining pixels are those whose values are greater than the threshold in all of the three channels. This is possible given that clouds present similar values on the three considered wavelengths, reflecting a similar amount of energy in any of them.

After the segmentation is performed, a cloud index coefficient $n(i, t)$ is calculated. This coefficient is estimated for the pixel of interest as the fraction between a minimum value in each of the channels in the original image (no cloud reflection) and the maximum value that corresponds to a white intense cloud. It is important to note, that the water masses absorb the majority of incident energy, so the ocean was ignored given that our interest is the continental territory, therefore the minimum value corresponds to a minimum pixel intensity value of a continental location. The cloud index is calculated from these two values and the desired pixel intensity as proposed by Boulifa et al. [2015] and depicted on equation 3.1.

$$n(i) = \frac{C_i - C_{min}}{C_{max} - C_{min}} \tag{3.1}$$

Where *n(i)* corresponds to the cloud index for the i pixel, C_i, C_{max}, C_{min} correspond to the intensity level of the pixel i, the maximum intensity value of the image, and the minimum one, respectively. Once the cloud index has been calculated, the following step is to estimate the clear sky index, according to equation 3.2 proposed by Rigollier et al. [2004].

$$k_c = \begin{cases} 1.2 & \text{if } n \leq -0.2 \\ 1 - n & \text{if } n \in (-0.2, 0.8] \\ 2.0667 - 3.6667n + 1.6667n^2 & \text{if } n \in (0.8, 1.1) \\ 0.05 & \text{if } n \geq 1.1 \end{cases} \tag{3.2}$$

The obtained K_c is then substituted in equation 1.1 to obtain the estimated GHI according to the weather conditions depicted in the image and the estimated GHI_{clr}.

3.3.2 Neural Networks

A CNN architecture is proposed and tested in comparison to a MP network as proposed by Quesada-Ruiz et al. [2015] and Linares-Rodriguez et al. [2013]. For both architectures, the output is a single unit representing the GHI while the input is a satellite image crop or pixel corresponding to the location of interest and the clear sky term. The architectures follow the general form seen in Figure 3.4.

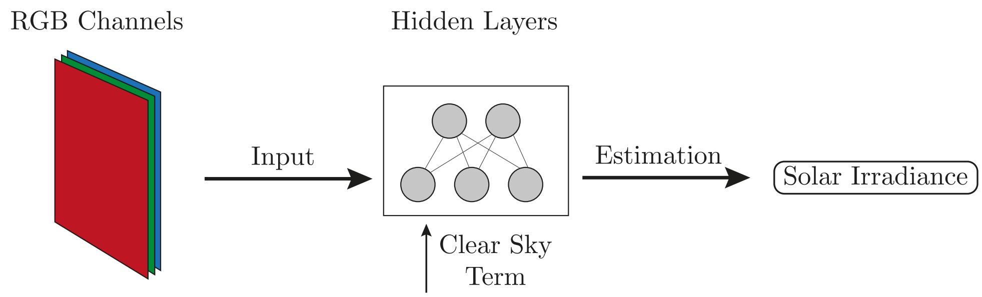

Figure 3.4: General structure of the proposed neural networks to estimate the GHI. The inputs are the RGB channels of the image crop and the clear sky GHI

In order to test the inclusion of neighbor pixels, the MP architecture is implemented with two different input conditions. In the first case only the corresponding pixel is counted following Quesada-Ruiz et al. [2015] and Linares-Rodriguez et al. [2013] implementation, with the difference of only taking into account the 3 visible channels (instead of 11). Therefore, a total of 4 independent inputs parameters are considered in this case (the 3 RGB channels and the corresponding pixel clear sky GHI). In the second case, in order to include the effect of neighbor pixels, an image crop of 15x15 pixels (as shown in Figure 3.3) is taken into account. Hence, a total of 676 independent inputs is considered in this situation (3 channels for each of the 225 pixels and the clear sky term).

The CNN architecture is also tested with the same 676 inputs of the aforementioned MP. More specifically, this CNN includes one convolutional layer with kernel size 2, stride 1 and 16 output channels with the Rectified Linear Unit (ReLU) as the activation function. This layer is followed by an average pooling layer with kernel size 3 and stride 2, finally closed by a fully connected layer with 10 neurons.

Both MP cases include one hidden layer with 10 neurons also using ReLU activation function.

3.4 Results

Two scenarios are defined to test the results: instantaneous GHI every 10 minutes and hourly average GHI computed from 6 instantaneous samples. Six different methods for estimating the GHI are tested:

1. ClrSky - Clear Sky Model (ESRA)
2. SClrSky - Scaled Clear Sky obtained by multiplying the ClrSky by the average ratio of the measured GHI and the clear sky GHI over the training data, this factor is 0.8291.
3. ImProc - Image Processing technique as explained in Section 3.3.1
4. CNN - Convolutional neural network with 15x15 pixel crop and the clear sky GHI as input, as explained in Section 3.3.2
5. MP1px - MP neural network with 1 pixel and the clear sky GHI as input, as explained in Section 3.3.2
6. MP15px - MP neural network with 15x15 pixel crop and the clear sky GHI as input, as explained in Section 3.3.2

The results are compared using the Mean Bias Error (MBE), the Root Mean Square Error (RMSE) and the normalized RMSE (nRMSE) in percentage. Equations 3.3, 3.4 and 3.5 describe their calculations. GHI, $\widehat{GHI}$ are the observed and estimated values correspondingly, $\overline{GHI}$ is the average of the observed values and n stands for the total number of observations.

$$MBE = \frac{1}{n}\sum_{i=1}^{n}(GHI_i - \widehat{GHI}_i) \tag{3.3}$$

$$RMSE = \sqrt{\frac{\sum_{i=1}^{n}(GHI_i - \widehat{GHI}_i)^2}{n}} \tag{3.4}$$

$$nRMSE = \frac{RMSE}{\overline{GHI}} * 100 \tag{3.5}$$

These errors are computed over the 13755 observations defined as testing data. Obtained results can be seen in Table 3.1.

The comparison between the observed and estimated GHI for a clear sky day and cloudy day for 10 minute sampling is depicted in Figure 3.5, the corresponding comparison for hourly average GHI of the same days is depicted in Figure 3.6.

	10 minute			Hourly		
	MBE	**RMSE**	**nRMSE**	**MBE**	**RMSE**	**nRMSE**
Method	(Wm^{-2})	(Wm^{-2})	(%)	(Wm^{-2})	(Wm^{-2})	(%)
ClrSky	-91.9	217.5	45.1	-95.5	196.5	39.2
SClrSky	6.2	188.6	39.1	6.5	162.3	32.4
ImProc	-70.2	186.4	38.7	-72.8	155.6	31.0
CNN	-10.5	129.9	27.0	-10.6	78.6	15.7
MP1px	12.0	140.1	29.1	12.6	87.3	17.4
MP15px	-1.7	130.4	27.1	-1.2	79.5	15.9

Table 3.1: GHI Estimation errors for the 6 different methods and 2 different scenarios: instantaneous GHI for every 10 minutes (left columns) and Hourly average GHI (right columns).

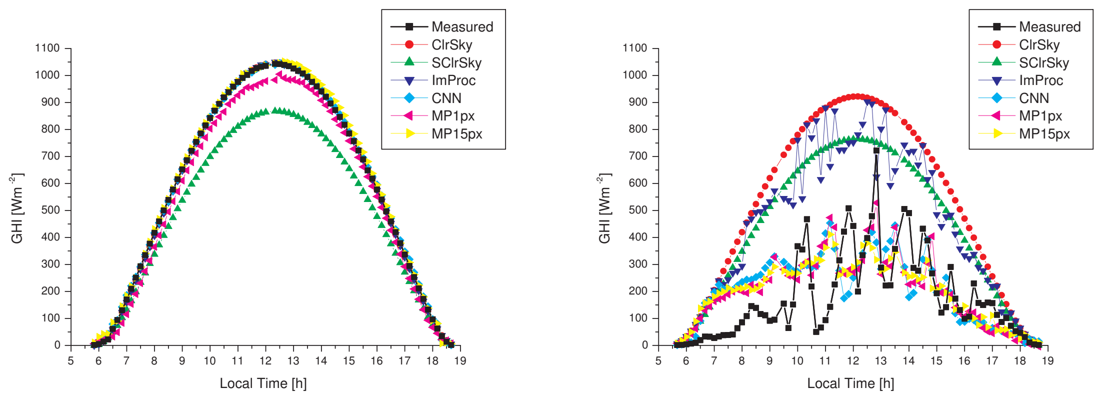

Figure 3.5: 10-minute measured and estimated GHI for a clear sky day on Alice Springs during October 15, 2015 (Left) and a cloudy day on Melbourne during October 12, 2015 (Right)

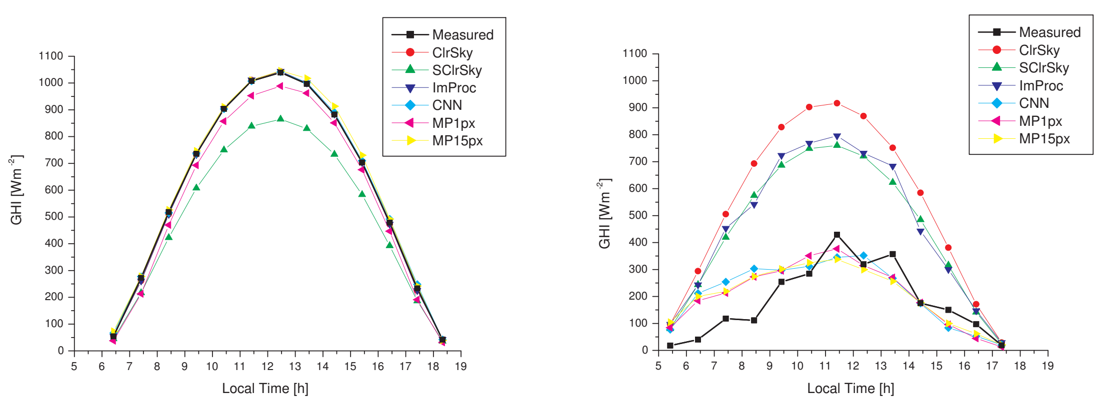

Figure 3.6: Hourly average from measured and estimated GHI for a clear sky day on Alice Springs during October 15, 2015 (Left) and a cloudy day on Melbourne during October 12, 2015 (Right)

3.5 Conclusions

As reported in literature, the satellite images include useful information in order to reduce the uncertainty on the solar GHI estimation. For the Australian continent satisfactory results are achieved using artificial intelligence techniques and Himawari-8 visible range satellite images.

Neighbor pixels included on the MP neural networks improved the estimation accuracy with respect to using only the corresponding pixel. The high resolution of the used images (1km x 1km per pixel) demands the consideration of neighbor pixels to identify clouds located more than 1km away, that may still affect the local GHI.

The CNN and the MP15px neural networks present very similar performance on the estimations, taking into account that both of them consider exactly the same input parameters. The MBE suggests a slight difference in favor of the MP15px. A computational efficiency test may be a second comparison factor.

The MBE obtained with the ClrSky and the ImProc methods shows that these estimations are, on average, much greater than the observations, this may induce to large errors on the calculations of solar energy received in larger time samples based on these estimations.

As depicted in Figures 3.5 and 3.6, the estimation error is greater on cloudy days, on clear sky days the estimation is more precise. The increase of the sampling time yields a decrease on the RMSE errors due to the smoothing of the curve and reduction of noise of the variables.

Compared to the results reported by Quesada-Ruiz et al. [2015], a similar RMSE is achieved on the hourly estimation using only the 3 visible range bands from the satellite images and more pixels.

Chapter 4

Solar car energy management for the WSC 2015

4.1 Introduction

The energy management optimization model is used to define the race strategy of the "EPM-EAFIT PRIMAVERA 2" solar car on the WSC version of 2015. This vehicle is designed and built according to the competition regulations with the main objective of minimizing the energy consumption at high speed and maximizing the energy capture from the sun while guaranteeing the reliability and safety of the driver. The vehicle is depicted in Figure 4.1.

Figure 4.1: PRIMAVERA 2 solar car, designed and built in EAFIT university by the EPM-EAFIT solar car team on 2015.

In this chapter, the strategy calculation and execution is widely described, the methodology used is based on the methods and conclusions presented in the two previous chapters. The experimental results are analyzed and the unexpected events are listed. Finally, The race performance is compared to the strategy plan.

The stochastic nature of climatic variables (e.g. GHI and wind) and the possibility of other random events (e.g. road work, traffic or vehicle failures) generate an uncertainty to define the exact strategy for solar cars before the WSC race. As found in the literature and clarified in the chapters 1 and 2, the race strategy must be recalculated frequently during the race according to the current state and new estimates of future variables.

The 2015 WSC race was started from Darwin on October 18 at 8:15 am with the goal of reaching Adelaide by traveling 3022 kilometers through the Stuart Highway in the shortest possible time. The strategy for this race (as defined in chapters 1 and 2) is posed as an optimization problem where the speed of the vehicle must be chosen at each moment to minimize the total race time, and subject to different optimization constraints.

Concerning the weather, the race strategy planning demands a prediction of the solar radiation that the vehicle will receive during the 5 or 6 days that it should take to travel. As described in the chapters 1 and 3, the prediction of this variable in the short or medium term includes an error that increases with the size of the time frame to be predicted. Therefore, no team is completely aware of the climatic conditions of the race before starting.

After the vehicle characterization, its main properties are validated in simulations and a race plan is executed to define the strategy and estimate its performance in the race. For this, two climatic conditions are proposed: an optimistic one considering clear sky conditions and a more realistic one based on the scaled clear sky radiation that was calculated in chapter 3.

In this chapter, the strategy planning process is explained as follows. Section 4.2 exposes the input data for the model, including the vehicle properties and the radiation scenarios. Section 4.3 briefly describes the methodology used for the race strategy optimization. Section 4.4 shows the optimal strategies found according to the inputs used. The real performance of the vehicle in race is presented in Section 4.5.3 and conclusions are listed in Section 4.5.

4.2 Data

The input data for the optimization algorithm is divided in two main groups: the vehicle properties and the environment data (See Figure 2.2).

4.2.1 Vehicle properties

Concerning the vehicle data, several experiments as recommended by Boulgakov [2012] were executed as well as solar panel testing. The aerodynamic characterization was done experimentally rather than using CFD results, this allowing possible shape alterations as explained in Betancur et al. [2017a]. The resulting properties used for the model are listed in table 4.1.

Battery Capacity [Wh]	5100
Crr, Roll coefficient [adim]	0.005
CdA, Drag Area coefficient [m2]	0.102
Vehicle mass [kg]	283
Regenerative brake efficency [adim]	0.4
Solar panel area free of shades [m2]	4.4926569
Solar panel area with canopy shades [m2]	1.4566635
Solar panel effiency [adim]	0.15
Drivetrain efficiency [adim]	0.97
Battery efficiency [adim]	0.9

Table 4.1: “Primavera 2” solar car properties used for the WSC 2015 strategy program

4.2.2 Climatological data

The environmental inputs required for the model are the air density (See Equation 2.1), the wind velocity in the forward direction (See Equation 2.1), the solar irradiance (See equation 2.3) and the sun elevation angle (See equation 2.3). These 4 variables are spatial and time dependant, nevertheless small variation on the air density allows its definition as constant, with a value of 1.185 kg/m^3.

The road is divided in 3022 sections (of 1km each) as a discretization of the spatial dimension. The wind velocity in the forward direction of the road is assumed constant in time and is calculated for every section using the monthly average (based on historical data) reported online by the Australian Government Bureau of Meteorology (Australian Government, Bureau of Meteorology [2017]) for certain weather stations. The wind direction and speed statistics for October is used to define the most likely wind vector for the locations listed in Table 4.2. Finally, a linear interpolation is used to estimate the wind vector for the 3022 race sections.

Regarding the solar variables, the sun position is calculated during the simulation for every road section based on the geographic location, date and exact time using the Sun-position algorithm proposed by Blanco-Muriel et al. [2001] due to its ease of use and efficiency.

Station	km
Darwin	0
Pine Creek	225
Katherine	317
Daly Waters	590
Elliot	735
Tennant Creek	989
Barrow Creek	1194
Alice Springs	1496
Kulgera	1785
Marla	1950
Coober Pedy	2183
Port Augusta	2723
Adelaide	3022

Table 4.2: Weather stations with historical wind data and corresponding location on race (in kilometers).

The solar irradiance is defined using the GHI as explained in Chapter 3. Two scenarios are defined according to the results reported in Section 3.4, a Clear Sky GHI (ClrSky) calculated using the ESRA model (Rigollier et al. [2000]) and a Scaled Clear Sky GHI (SClrSky) obtained by multiplying the clear sky by the attenuation factor of 0.8291 obtained in Chapter 3. The estimated GHI for the 3022 km and the first 6 days of race for both cases is displayed in figure 4.2.

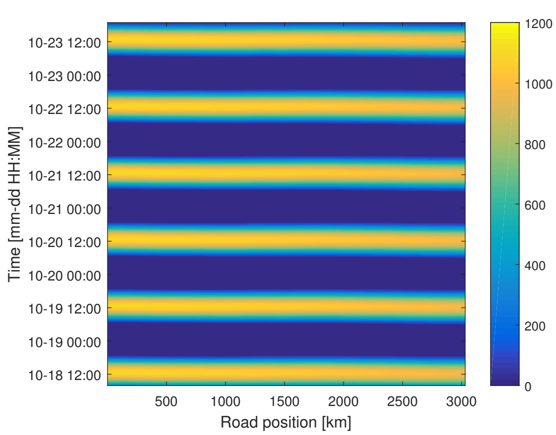

Figure 4.2: Estimated GHI for the 3022 kilometers and the first 6 days of race of the WSC 2015, using the ClrSky (left) and the SClrSky method (right).

4.3 Methodology

The optimal racing strategy is calculated using the race simulation program and the genetic algorithm optimization method for the race divided in 10 segments of constant speed between control stops. Please refer to Sections 2.2 and 2.3 for more information regarding the race simulation and the optimization method.

According to the two different irradiance predictions described in Section 4.2, two strategies are calculated, the other input data for both strategies is maintained constant. After the comparison of the resulting strategy plans, one of the two strategies is selected based on the analysis of recent satellite images and short term weather predictions (obtained from external weather reports) for the first section of the race.

Owing to the lack of information to predict random stops or failures, the race strategy is calculated excluding these events and a complete recalculation of the optimal strategy is recommended if they significantly affect the strategy plan execution.

As explained above, the optimization method is executed prior to the race to define the initial strategy. During the race, the strategy is recalculated on the night stops if several deviations from the previous strategy are noticed. For the recalculation, different parameters are updated according to the vehicle performance, the solar panel efficiency, the drag area coefficient and the roll coefficient may be updated using historical data from the race. The information collected from the race is considered as the most recent and valid test of the vehicle, therefore the vehicle parameters are updated for the strategy recalculations using this race data.

After the race, the experimental results are compared to the strategy plan. The main race variables to compare are velocity and SOC with respect to the race position (kilometer) and race position with respect to the time. Moreover, using the satellite image based convolutional neural network procedure described in Chapter 3, the real radiation is estimated after the race and compared to the radiation predicted on the optimization model.

4.4 Results

4.4.1 Optimization results

The main results of the initial strategies calculated for the two irradiance cases are presented in Table 4.3. A difference of 3.1 race hours (7.4%) is obtained from both strategies. Although it may seem insignificant, this difference represents reaching the finish line a day later and very likely some positions in the race results.

A more detailed description of both strategies is presented in Figure 2.5. The ClrSky case that considers a higher energy input, suggests a higher velocity and, therefore, a shorter race time. The suggested velocity in this case is maintained with few variations during the race ranging from 77 to 86 km/h. On the other hand, the SClrSky may be considered a more conservative strategy where less energy is obtained from the solar panel and more energy is saved for the last 300 km of the race where the velocity is increased, taking advantage of the energy captured in the extra night. In this case the velocity is maintained between 70 and 76 km/h until the last section of the race where is increased to 88 km/h. Although, both strategies tend to finish the race with empty battery, this second one leaves almost 20% of the SOC due to the energy obtained on the last day end stop.

The strategy to be used is selected based on different insights of the future irradiance. Although some prediction approaches, as the ones mentioned in Section 1.4.2, might have reduced the uncertainty for a short term future (at least a couple of days), the project scope and schedule made its implementation unfeasible. According to the satellite images obtained prior to the race start (e.g. Figure 4.4.1), clear sky conditions prevailed for the north of Australia, corresponding to the first part of the race. Therefore, the selected initial strategy is the first one exposed considering the ClrSky irradiance.

Radiation input	**Race time [h]**	**Arrival day [#]**	**Arrival time [hh:mm]**
ClrSky	41.91	5	14:53
SClrSky	45.01	6	08:59

Table 4.3: Main results of optimal strategies considering clear sky and scaled clear sky conditions. The race time includes all the 30-minutes control stops.

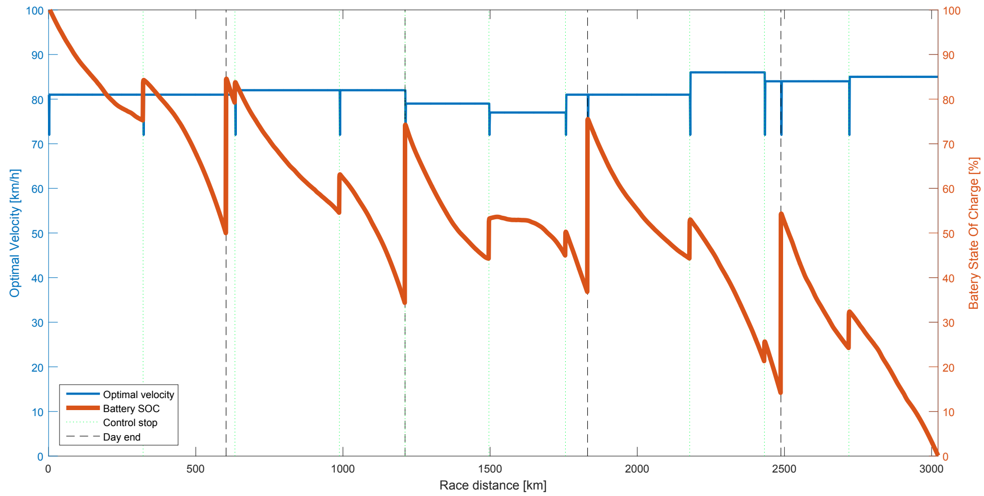

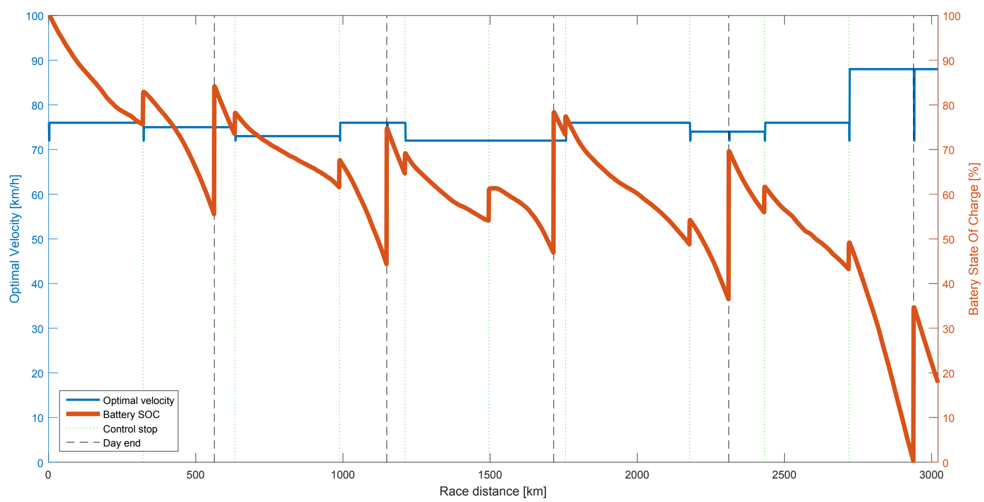

Figure 4.3: Optimal strategy represented by the state of charge of the battery and velocity vector for different environmental conditions: ClrSky (Top) SClrSky conditions (Bottom). The control stops (dotted lines) indicate 30 min mandatory stops, the discontinuous black lines indicate the km where the night is spent.

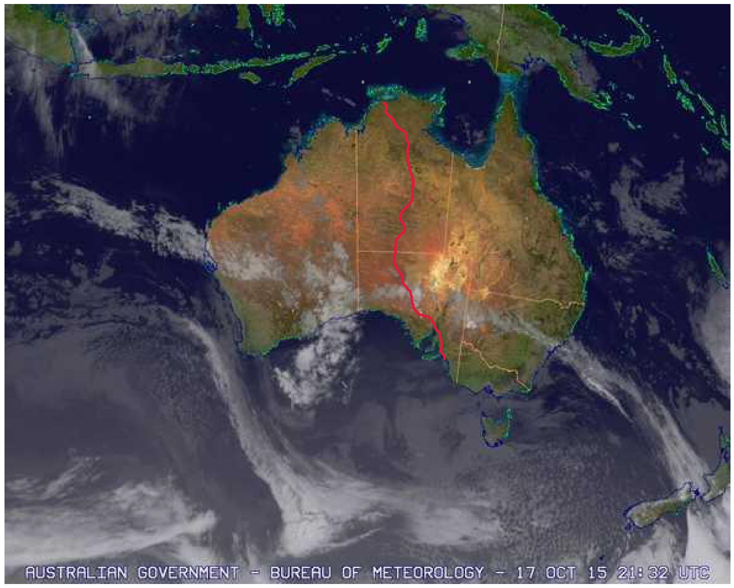

Figure 4.4: Satellite image of Australia taken on October 18 at 7:32 AM (Darwin time). The race start is in Darwin (North) and the road is described by the red line. (Image obtained from `http://www.bom.gov.au/australia/satellite/`)

4.4.2 Experimental results

Experimental results exposed in this section correspond to the real performance of the vehicle during the 2015 WSC. The vehicle main variables (e.g. position, velocity, SOC, panel power, motor power, etc.) are measured and stored every minute. The cruising velocity may be set on the vehicle cruise control but several disturbances were found due to traffic conditions, road turns, winds or vehicle minor failures, therefore the average velocity between stops is used to compare the results.

As explained in Section 4.4.1, the strategy considering ClrSky irradiance is selected to begin the race. According to this strategy, an optimal cruising velocity is defined and an estimated battery SOC curve should be accomplished. Once in race, constant control of three variables is made: SOC, velocity and position. This, in order to analyze the deviations from the defined strategy and propose corrections on the velocity. The SOC and velocity are plotted for every position on race (i.e. kilometer) in Figure 4.5 while the position is plotted for the time of the day in Figure 4.6.

Four unexpected events happened during the race:

1. High traffic of vehicles and solar cars was witnessed on the first 300 km after the departure. This can be seen on the velocity plot of Figure 4.5 where the average speed for the first section is lower than the suggested one.

2. A strong gust of lateral wind in km 800 pushed the vehicle out of the road an a

45-minute stop to repair and check the vehicle was forced. After this stop, the SOC was 15% higher than the expected for the same km and the vehicle was 1 hour delayed with respect to the strategy plan (see Figures 4.5 and 4.6). Although the recommended solution is to completely recalculate the strategy in this moment, it resulted impossible due to logistical and software limitations. Therefore, the velocity was incremented in order to recover time.

3. A failure in the connection of a solar panel cable caused the loss of 33% of the solar panel between hours 13:00 and 16:40 of the third day, corresponding to the section between km 1496 and 1756. The failure was solved and the panel was 100% functional from there on.

4. Strong headwinds and high traffic in the afternoon of the fifth day, after km 2719, forced the vehicle to slow down until the night stop.

The race strategy is fully recalculated in km 1756 during the third night stop after solving the failure on the solar panel connection (see Figures 4.5 and 4.6). For this strategy recalculation the vehicle CdA is changed from 0.102 to 0.12 m^2 according to the consumption observed during the previous days, the other input data for the simulation including the solar irradiance remained constant. This new strategy includes the current SOC, position and time as an input and using the same optimization algorithm provides the optimal speed for the remaining sections of the race. A comparison between the main results of the initial and recalculated strategies is presented in Table 4.4.

	Race time [h]	**Arrival day [#]**	**Arrival time [hh:mm]**
Initial strategy	41.91	5	14:53
Recalculated strategy	43.20	5	16:10
Race results	46.32	6	09:47

Table 4.4: Main results of the optimal strategies used and the final race performance. Both strategies consider clear sky conditions. The race time includes all the 30-minutes control stops.

After the strategy recalculation on km 1756, the SOC prediction for every km is followed while the vehicle average velocity remains lower than the desired one (See Figure 4.5). This lower velocity leads to an incremental delay with respect to the strategy plan. The last control stop in km 2719 is achieved at 13:07 of the fifth day, 1 hour and 17 minutes later than the expected. This delay summed to the the high traffic and headwind conditions on the afternoon of day 5 forces an extra night stop before the race end. The fifth night stop at km 2985 provides enough energy for the remaining 127 km to the end, allowing to finish the race at 09:47 in the morning of the sixth day with a remaining 20% of the battery SOC.

The race is finished in the ninth position among 29 participants in the Challenger class. The first vehicle (Nuon Solar Team from TU Delft, Netherlands) finished the race in the morning of the fifth day with a total race time of 37.93 h, resulting 8.42 racing hours ahead.

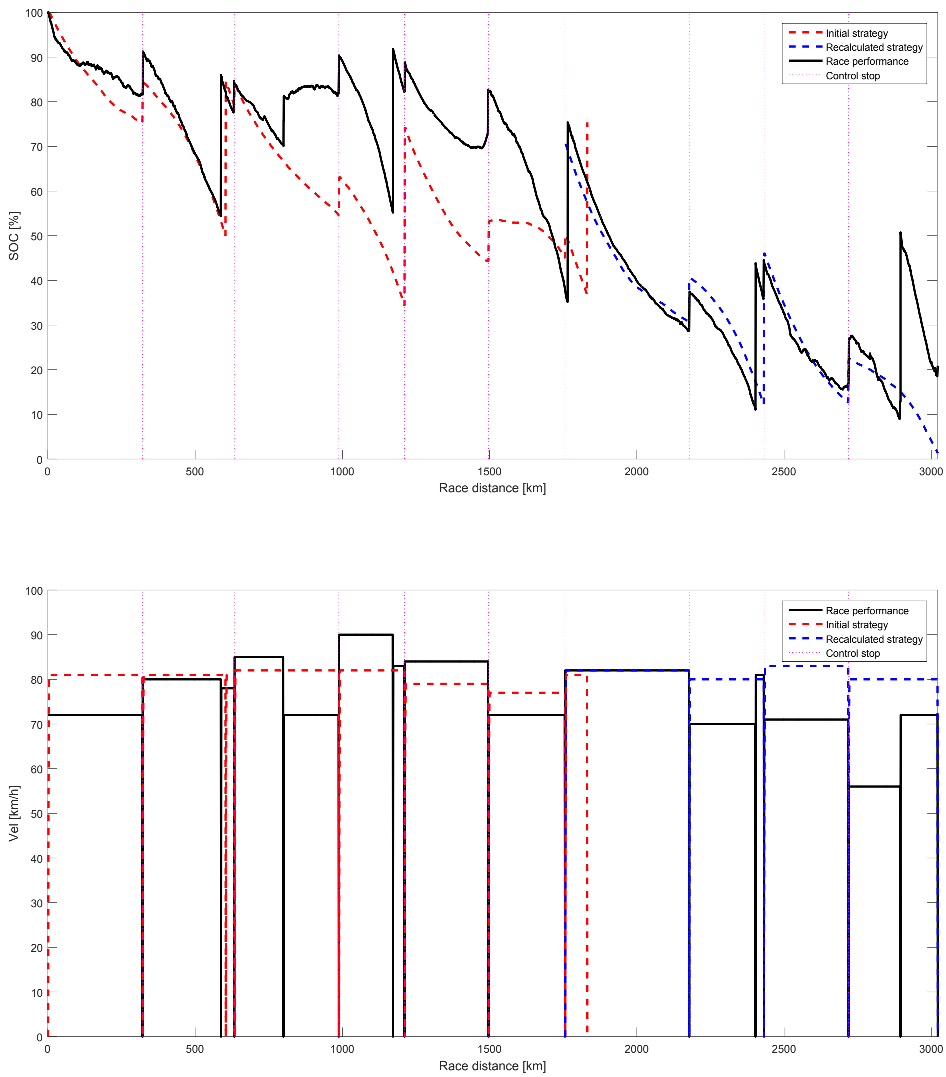

Figure 4.5: Race performance and racing strategy represented by the continuous and dashed lines respectively. The plots indicate the state of charge of the battery (Top) and vehicle velocity (Bottom) for the entire race. The race velocity plot is the average between successive stops.

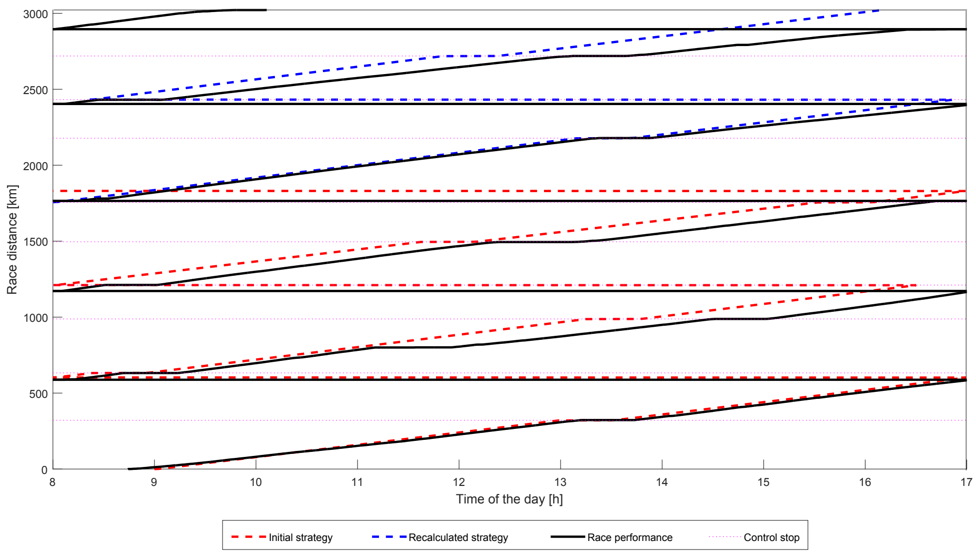

Figure 4.6: Race performance and racing strategy represented by the continuous and dashed lines respectively. The plot indicates the position (in kilometers) for every time of the racing days.

In order to validate the irradiance input used, the real GHI for the 3022 km and the first 6 days of race is calculated after the race using the corresponding series of satellite images and the ClrSky estimation on the convolutional neural network algorithm (CNN) presented in Chapter 3. A total of 786 RGB satellite images with a 10-minute sampling time are used. The race distance is divided in 3022 sections and the GHI is obtained for every image and kilometer. The vehicle position on the resulting irradiance map is presented in Figure 4.7.

The ClrSky and SClrSky models used in the strategy program are compared to the CNN estimated GHI for the positions of the vehicle in race. Figure 4.8 compares the irradiances obtained using the vehicle position on the GHI distributions presented in Figures 4.2 and 4.7. The MBE, RMSE and nRMSE errors (defined in Section 3.4) between both predictions and the CNN estimation are shown in table 4.5.

	MBE Wm^{-2}	**RMSE** Wm^{-2}	**nRMSE** (%)
ClrSky	19.68	94.65	11.57
SClrSky	-143.69	171.66	20.99

Table 4.5: Estimation errors for the ClrSky GHI with respect to the calculated CNN GHI.

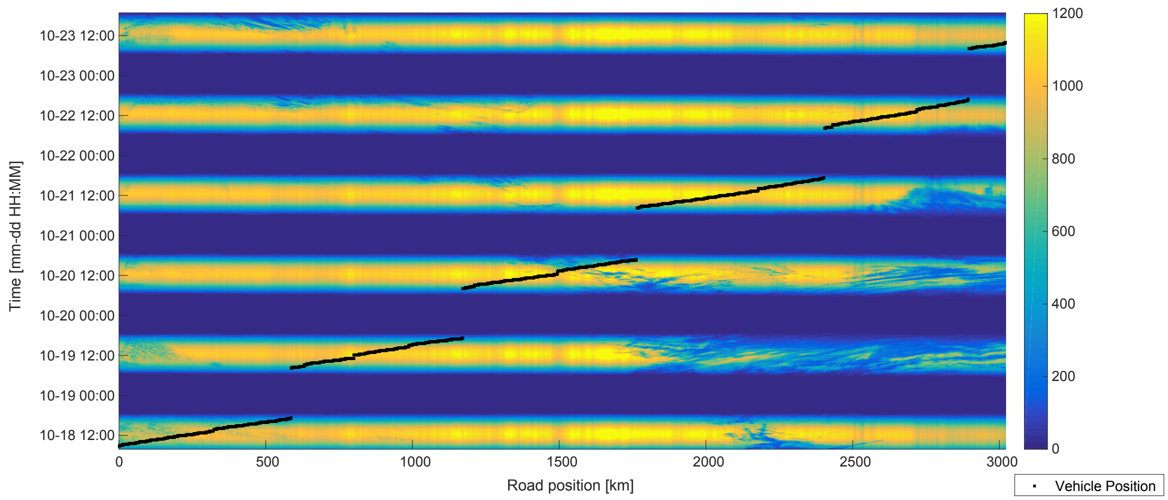

Figure 4.7: Global Horizontal Irradiance calculated after the race using satellite images and CNN for the 3022 kilometers and the 6 days of the WSC 2015. The vehicle position during the race is described by the black line.

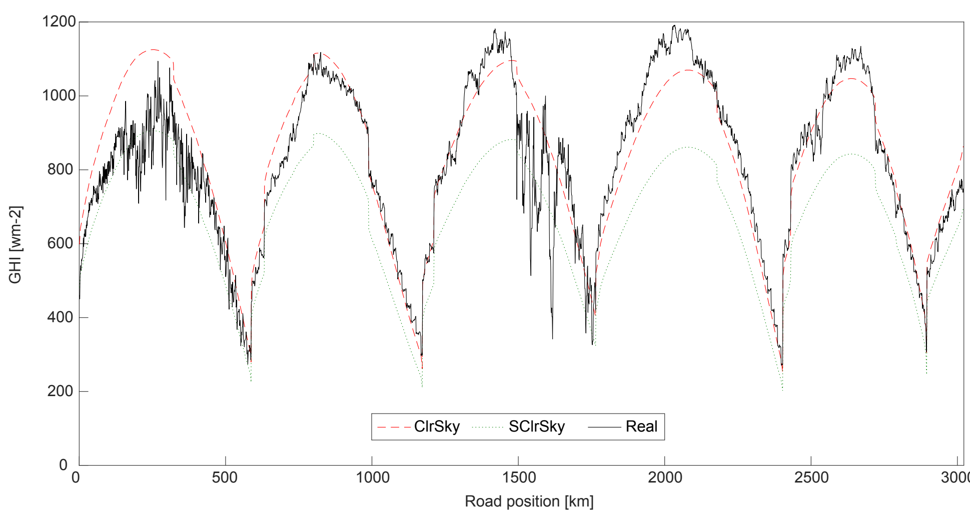

Figure 4.8: Global Horizontal Irradiance according to the vehicle position in race. The ClrSky GHI is calculated prior to the race and used in the strategy program, the CNN GHI is estimated after the race using satellite images.

4.5 Conclusions and perspectives

An optimization method for solar cars racing strategy is proposed, implemented, tested and validated. The inclusion of stochastic variables is discussed and special emphasis is made on the solar irradiance prediction and estimation using satellite images. Artificial intelligence techniques are used for the optimization algorithm (heuristic optimization methods) and the solar irradiance estimation (machine learning) with satisfactory results. The proposed method is experimentally validated in the 2015 World Solar Challenge race in Australia, the strategy plan and real results are compared and discussed. Satisfactory results are obtained using the race strategy although unexpected and unpredictable events occurred during the race.

4.5.1 Heuristic optimization method

Calculated optimal strategies may be considered as the optimal energy management plan, where the available energy is cleverly used to minimize the racing time. This explains why all the calculated optimal strategies aim to finish the race with the empty battery. As discussed in Chapter 2, the calculated strategy is not the global optimum for the given inputs. This is caused by two main factors, the assumption of constant velocity between control stops that limits the search space to 10-dimensional vectors and, in the other hand, the use of an heuristic optimization method that results in non global-optimum solutions. Regarding the race division in 10 segments with constant velocity, the high computational cost of optimizing for finer segment divisions, compared to the possible small improvement in the objective function (as the one stated with the change of 3D to 10D vectors in Chapter 2), makes this refinement a non cost-effective solution. Although, the genetic algorithm method used for the optimization may not calculate the global optimum, the monotonic convergence reported in Chapter 2, added to the randomness nature of the optimization process, guarantees the validity of the obtained solution.

4.5.2 Meteorological prediction

The vehicle and environmental data used as input for the optimization model defines the resulting optimal strategy as it is proved in Chapters 2 and 4. A high sensitivity to changes in solar radiation is appreciated in Table 4.3 and Figure 2.5, where a reduction of 17% on the solar irradiance prediction leads to an increment of 7.4% on the total race time, an average reduction of 8.2% on the optimal velocity and an extra night stop on race. This difference on the solar irradiance is obtained using the ClrSky and SClrSky assumptions described in Chapter 3. The sensitivity of the optimal strategy with respect to other variables may be calculated, as reported for the irradiance, by inducing variations on the input data and comparing the obtained solutions.

Selecting the appropriate inputs for the strategy involves the prediction of uncertain meteorological variables (i.e. solar irradiance and wind velocity) that affect the energy consumption and intake, as it is exposed in Section 2.2. Special effort must be made on the study of the solar irradiance and wind vectors to make clever decisions when predicting their values for the entire race. Prior to the race, two options for the solar radiation input were considered, the ClrSky assuming that no clouds would be present during the entire race and the SClrSky considering that clouds would be present and the received irradiance is scaled according to the average of historical data. These assumptions may be considered as optimistic and conservative cases for the strategy. In this case, the ClrSky was selected following external forecasts and satellite image sequences just before the race. This may be considered a successful decision given that there were no cloudy days during the race as reported in Table 4.5 and Figures 4.7 and 4.8.

The use of machine learning procedures to estimate the solar irradiance from satellite images produced satisfactory results, as it is stated in Chapter 3. Although approximation errors, as the ones mentioned in the state of the art, were obtained, the Convolutional Neural Networks resulted in a suitable method for this regression problem. As reported in Section 1.4, satellite images are also used to predict short-term future radiation, however the implementation of this procedure is left as future work due to the limited scope of the project.

4.5.3 Experimental results

A 3022 kilometer race is an endurance challenge for a prototype vehicle and a team. The fact of racing during more than 5 continuous days from 8:00 to 17:00 brings with it the possibility of having unexpected and unpredictable events at any time. In this case the wind gust that caused the 45-minute stop and the loss of a third of the solar panel during 4 hours were the two main unexpected events that affected the strategy plan. In the other hand, non-predicted winds that caused higher energy consumption and high traffic in urban areas may be considered other unexpected factors.

The strategy recalculation during the race is the proposed solution to unexpected deviations on the strategy plan. Although, an efficient and automatic manner of recalculating the race strategy was not implemented for this race, the strategy was successfully recalculated on km 1756. Special effort must be made on solving this necessity to be able to make clever decisions rapidly.

Following the race strategy requires keeping track of two main variables, the race position with respect to the time and the battery SOC with respect to the position, while the velocity is the control variable. As stated in Chapter 2 and 4, in most of the cases an optimal race strategy meets two conditions, finishing the race with empty battery and homogeneous (near constant) velocity for all the race (see Figures 2.5 and 4.3). The results reported in Figure 4.5 suggest that the strategy followed in the race approaches these conditions.

The 8.42 hours difference between the own result and the first vehicle to finish may be attributed to several causes apart from the strategy itself: a more energy-efficient vehicle both in consumption and collection, a more accurate prediction of the weather conditions, the different unexpected events and the position in the starting grid. It can be seen that the initial strategy using optimistic weather predicted a race time of 41.91 h, still greater than the winner time (37.93 h).

The solar irradiance received by the vehicle during the race was barely affected by clouds, therefore the ClrSky model was the most approximate prediction of this variable (See Figure 4.8). Nevertheless, for future cases no generalizations must be assumed due to the randomness nature of the weather, a completely cloudy day may induce several variations as reported in Chapter 2.

Although a high correlation on the SOC distribution and total race time may be appreciated between the calculated strategy considering SClrSky GHI (Figure 4.3) and the race results (Figure 4.5), where both include a fifth night stop near the finish line, there is no causal relationship between them. As mentioned above, the race delays are attributed to random events apart from the GHI, and the most approximate model to the received irradiance on race was the ClrSky.

4.5.4 Future work

As future work, the solar irradiance prediction for a short term future is proposed. The satisfactory results obtained on the GHI estimation using deep learning procedures with satellite images, suggest that these techniques, together with cloud motion estimation, may give accurate GHI predictions according to the necessities on solar car racing.

On the other hand, the implementation of this strategy program with a user-friendly interface and high computational efficiency will result in a tool that makes the difference in solar vehicle races.

The experimental validation of this model is suggested in new races. For instance, the Cruiser class of the recent WSC forces modifications on the optimization function and control variables as it includes variable battery size, number of occupants and charging stops. Nevertheless, the structure of the vehicle model and optimization algorithm proposed may be applied to this case.

Bibliography

R Al Zaher. Axial flux permanent magnet motor csiro. Master's thesis, Delft University of Technology, 2010.

Erkan Atmaca. Energy management of solar car in circuit race. *Turkish Journal of Electrical Engineering & Computer Sciences*, 23(4):1142–1158, 2015.

Australian Government, Bureau of Meteorology. Climate and oceans data and analysis. `http://www.bom.gov.au/climate/data/stations/`, 2017. Accessed: 2017-03-24.

Esteban Betancur, Cristiano Fragassa, Jairo Coy, Sebastian Hincapie, and Gilberto Osorio-Gómez. Aerodynamic effects of manufacturing tolerances on a solar car. In *International Conference on Sustainable Design and Manufacturing*, pages 868–876. Springer, 2017a.

Esteban Betancur, Ricardo Mejía-Gutiérrez, Gilberto Osorio-Gómez, and Alejandro Arbelaez. Design of structural parts for a racing solar car. In *Advances on Mechanics, Design Engineering and Manufacturing*, pages 25–32. Springer International Publishing, 2017b.

Esteban Betancur, Gilberto Osorio-Gómez, and Juan Carlos Rivera. Heuristic optimization for the energy management and race strategy of a solar car. *Sustainability*, 9(10):1576, 2017c.

Manuel Blanco-Muriel, Diego C Alarcón-Padilla, Teodoro López-Moratalla, and Martín Lara-Coira. Computing the solar vector. *Solar Energy*, 70(5):431–441, 2001.

Alexandra Boulgakov. Sunswift iv strategy for the 2011 world solar challenge. Master's thesis, University of New South Wales, 2012.

M Boulifa, A Adane, A Rezagui, et al. Estimate of the global solar radiation by cloudy sky using hrv images. *Energy Procedia*, 74:1079–1089, 2015.

Daniel Cano, Jean-Marie Monget, Michel Albuisson, Hervé Guillard, Nathalie Regas, and Lucien Wald. A method for the determination of the global solar radiation from meteorological satellite data. *Solar Energy*, 37(1):31–39, 1986.

CS Chang and SS Sim. Optimising train movements through coast control using genetic algorithms. *IEE Proceedings-Electric Power Applications*, 144(1):65–73, 1997.

John Connors. On the subject of solar vehicles and the benefits of the technology. In *Clean Electrical Power, 2007. ICCEP'07. International Conference on*, pages 700–705. IEEE, 2007.

Michael W Daniels and PR Kumar. The optimal use of the solar powered automobile. *IEEE control systems*, 19(3):12–22, 1999.

Vincent de Geus. World solar challenge: the race strategy explained. *ACM SIGEVOlution*, 2(3):2–5, 2007.

Ignacio de Los Rios, Adolfo Cazorla, José M Díaz-Puente, and José L Yagüe. Project–based learning in engineering higher education: two decades of teaching competences in real environments. *Procedia-Social and Behavioral Sciences*, 2(2):1368–1378, 2010.

NA Engerer and FP Mills. Validating nine clear sky radiation models in australia. *Solar Energy*, 120:9–24, 2015.

Osman K Erol and Ibrahim Eksin. A new optimization method: big bang–big crunch. *Advances in Engineering Software*, 37(2):106–111, 2006.

Andre Esteva, Brett Kuprel, Roberto A Novoa, Justin Ko, Susan M Swetter, Helen M Blau, and Sebastian Thrun. Dermatologist-level classification of skin cancer with deep neural networks. *Nature*, 542(7639):115–118, 2017.

Nima Ghaviha, Markus Bohlin, and Erik Dahlquist. Speed profile optimization of an electric train with on-board energy storage and continuous tractive effort. In *Power Electronics, Electrical Drives, Automation and Motion (SPEEDAM), 2016 International Symposium on*, pages 639–644. IEEE, 2016.

Gregor Giebel, Richard Brownsword, George Kariniotakis, Michael Denhard, and Caroline Draxl. The state-of-the-art in short-term prediction of wind power: A literature overview. *ANEMOS. plus*, 2011.

Teofilo F Gonzalez. *Handbook of approximation algorithms and metaheuristics*. CRC Press, 2007.

Enrique Guerrero Merino and Manuel A. Duarte-Mermoud. Online energy management for a solar car using pseudospectral methods for optimal control. *Optimal Control Applications and Methods*, 37(3):537–555, 2016. ISSN 1099-1514. doi: 10.1002/oca.2210. URL `http://dx.doi.org/10.1002/oca.2210`.

Enrique Eduardo Guerrero Merino. *Control óptimo de vehículos eléctricos con energía disponible restringida en ruta parcialmente conocida*. PhD thesis, Universidad de Chile, 2013.

Christian Gueymard. Critical analysis and performance assessment of clear sky solar irradiance models using theoretical and measured data. *Solar Energy*, 51(2):121–138, 1993.

Christian A Gueymard. Rest2: High-performance solar radiation model for cloudless-sky irradiance, illuminance, and photosynthetically active radiation–validation with a benchmark dataset. *Solar Energy*, 82(3):272–285, 2008.

Seong Ho Han, Yun Sub Byen, Jong Hyen Baek, Tae Ki An, Su Gil Lee, and Hyun Jun Park. An optimal automatic train operation (ato) control using genetic algorithms (ga). In *TENCON 99. Proceedings of the IEEE Region 10 Conference*, volume 1, pages 360–362. IEEE, 1999.

Mehrija Hasicic, Damir Bilic, and Harun Siljak. Criteria for solar car optimized route estimation. *Microprocessors and Microsystems*, 51:289–296, 2017.

Mohammad Havaei, Axel Davy, David Warde-Farley, Antoine Biard, Aaron Courville, Yoshua Bengio, Chris Pal, Pierre-Marc Jodoin, and Hugo Larochelle. Brain tumor segmentation with deep neural networks. *Medical image analysis*, 35:18–31, 2017.

John H Holland. *Adaptation in natural and artificial systems: an introductory analysis with applications to biology, control, and artificial intelligence.* U Michigan Press, 1975.

PG Howlett and PJ Pudney. An optimal driving strategy for a solar powered car on an undulating road. *Dynamics of]Continuous Discrete and Impulsive Systems*, 4(4): 553–567, 1998.

Phil Howlett. Optimal strategies for the control of a train. *Automatica*, 32(4):519–532, 1996.

Phil Howlett. The optimal control of a train. *Annals of Operations Research*, 98(1-4): 65–87, 2000.

Phil Howlett, Peter Pudney, Tania Tarnopolskaya, and David Gates. Optimal driving strategy for a solar car on a level road. *IMA Journal of Management Mathematics*, 8(1): 59–81, 1997.

Phil G Howlett, Peter J Pudney, and Xuan Vu. Local energy minimization in optimal train control. *Automatica*, 45(11):2692–2698, 2009.

Statistics IEA. Co2 emissions from fuel combustion 2017. Technical report, International Energy Agency, IEA, 2017.

Muhammad Iqbal. *An introduction to solar radiation.* Elsevier, 2012.

Hisao Ishibuchi and Tadahiko Murata. Multi-objective genetic local search algorithm. In *Evolutionary Computation, 1996., Proceedings of IEEE International Conference on*, pages 119–124. IEEE, 1996.

Japan Meteorological Agency. Himawari standard data user's guide. Technical report, Japan Meteorological Agency, Tokyo, 2017.

Jan Kleissl. *Solar energy forecasting and resource assessment*. Academic Press, 2013.

Alex Krizhevsky, Ilya Sutskever, and Geoffrey E Hinton. Imagenet classification with deep convolutional neural networks. In *Advances in neural information processing systems*, pages 1097–1105, 2012.

Bo Leckner. The spectral distribution of solar radiation at the earths surface-elements of a model. *Solar energy*, 20(2):143–150, 1978.

Yann LeCun, Yoshua Bengio, and Geoffrey Hinton. Deep learning. *Nature*, 521(7553): 436–444, 2015.

Alvaro Linares-Rodriguez, José A. Ruiz-Arias, David Pozo-Vazquez, and Joaquin Tovar-Pescador. An artificial neural network ensemble model for estimating global solar radiation from Meteosat satellite images. *Energy*, 61:636–645, 2013.

Shaofeng Lu, Stuart Hillmansen, Tin Kin Ho, and Clive Roberts. Single-train trajectory optimization. *IEEE Transactions on Intelligent Transportation Systems*, 14(2):743–750, 2013.

Ricardo Marquez, Hugo TC Pedro, and Carlos FM Coimbra. Hybrid solar forecasting method uses satellite imaging and ground telemetry as inputs to anns. *Solar Energy*, 92:176–188, 2013.

A Mefti, A Adane, and MY Bouroubi. Satellite approach based on cloud cover classification: Estimation of hourly global solar radiation from meteosat images. *Energy Conversion and Management*, 49(4):652–659, 2008.

Giangiacomo Minak, Cristiano Fragassa, and Felipe Vannucchi de Camargo. A brief review on determinant aspects in energy efficient solar car design and manufacturing. In *International Conference on Sustainable Design and Manufacturing*, pages 847–856. Springer, 2017.

Cristian Musardo, Giorgio Rizzoni, Yann Guezennec, and Benedetto Staccia. A-ecms: An adaptive algorithm for hybrid electric vehicle energy management. *European Journal of Control*, 11(4-5):509–524, 2005.

Aykut Ozgun Onol, Orhan Atabay, Arif Icke, and Onur Serin. Longitudinal dynamics simulation of a solar electric vehicle for driving strategy optimisation. *International Journal of Vehicle Design*, 73(1-3):136–156, 2017.

Nobuyuki Otsu. A threshold selection method from gray-level histograms. *IEEE transactions on systems, man, and cybernetics*, 9(1):62–66, 1979.

Sam Paterson, Pujith Vijayaratnam, Charith Perera, and Graham Doig. Design and development of the sunswift eve solar vehicle: a record-breaking electric car. *Proceedings of the Institution of Mechanical Engineers, Part D: Journal of Automobile Engineering*, pages 1972–1986, 2016.

Sophie Pelland, Jan Remund, Jan Kleissl, Takashi Oozeki, and Karel De Brabandere. Photovoltaic and solar forecasting: state of the art. *IEA PVPS, Task*, 14:1–36, 2013.

Peter Pudney. *Optimal energy management for solar-powered cars*. PhD thesis, University of South Australia, 2000.

Peter Pudney and Phil Howlett. Critical speed control of a solar car. *Optimization and engineering*, 3(2):97–107, 2002.

S Quesada-Ruiz, A Linares-Rodríguez, J A Ruiz-Arias, D Pozo-Vázquez, and J Tovar-Pescador. An advanced ann-based method to estimate hourly solar radiation from multi-spectral msg imagery. *Solar Energy*, 115:494–504, 2015.

REN21. Renewables 2017 global status report. Technical report, REN21 Secretariat, Paris, France, 2017.

Christelle Rigollier, Olivier Bauer, and Lucien Wald. On the clear sky model of the esra-european solar radiation atlas-with respect to the heliosat method. *Solar energy*, 68(1):33–48, 2000.

Christelle Rigollier, Mireille Lefèvre, and Lucien Wald. The method heliosat-2 for deriving shortwave solar radiation from satellite images. *Solar Energy*, 77(2):159–169, 2004.

D.M. Roche. *Speed of Light: The 1996 World Solar Challenge*. University of New South Wales Press, 1997.

Kumara Sastry, David E Goldberg, and Graham Kendall. Genetic algorithms. In *Search methodologies*, pages 93–117. Springer, 2014.

Alexander Scheidegger. Energy management optimization for a solar vehicle. Master's thesis, École Polytechnique Fédérale de Lausanne, 2006.

Xiaoyan Shao, Siyuan Lu, Theodore G van Kessel, Hendrik F Hamann, Leda Daehler, Jeffrey Cwagenberg, and Alan Li. Solar irradiance forecasting by machine learning for solar car races. In *Big Data (Big Data), 2016 IEEE International Conference on*, pages 2209–2216. IEEE, 2016.

Yasuo Shimizu, Yasuyuki Komatsu, Minoru Torii, and Masato Takamuro. Solar car cruising strategy and its supporting system. *JSAE review*, 19(2):143–149, 1998.

G. Tamai. *The Leading Edge: Aerodynamic Design of Ultra-streamlined Land Vehicles*. Engineering and Performance. Robert Bentley, 1999.

Shunsuke Tamura. Teijin's advanced carbon fiber technology used to build a car for the world solar challenge. *Reinforced Plastics*, 60(3):160–163, 2016.

Robert J Vanderbei. Case studies in trajectory optimization: Trains, planes, and other pastimes. *Optimization and Engineering*, 2(2):215–243, 2001.

Nikolay A Vinnichenko, Alexander V Uvarov, Irina A Znamenskaya, Herchang Ay, and Tsun-Hsien Wang. Solar car aerodynamic design for optimal cooling and high efficiency. *Solar Energy*, 103:183–190, 2014.

Raffaele Volpe, Valérie Ferrand, Arthur Da Silva, and Luis Le Moyne. Forces and flow structures evolution on a car body in a sudden crosswind. *Journal of Wind Engineering and Industrial Aerodynamics*, 128:114–125, 2014.

Cyril Voyant, Gilles Notton, Soteris Kalogirou, Marie-Laure Nivet, Christophe Paoli, Fabrice Motte, and Alexis Fouilloy. Machine learning methods for solar radiation forecasting: A review. *Renewable Energy*, 105:569–582, 2017.

Lucien Wald, Michel Albuisson, Clive Best, Catherine Delamare, Dominique Dumortier, Elena Gaboardi, Anette Hammer, Detlev Heinnemann, Richard Kift, Stefan Kunz, et al. Soda: a project for the integration and exploitation of networked solar radiation databases. In *Environmental Communication in the Information Society*, pages 713–720, http://www.soda-pro.com/help/general-knowledge/linke-turbidity-factor, 2002. International Society for Environmental Protection, Vienna, Austria.

World Solar Challenge. https://www.worldsolarchallenge.org Accesed July 2018, 2018.

Amit Kumar Yadav and SS Chandel. Solar radiation prediction using artificial neural network techniques: A review. *Renewable and Sustainable Energy Reviews*, 33:772–781, 2014.

Tsubasa Yamazakii, Hidekazu Uchiyama, Kazuaki Nakazawa, Tsubasa Isomura, and Hisashi Ogata. The development of direct drive motors for solar cars. Technical report, SAE Technical Paper, 2017.

Engin Yesil, Aykut Ozgun Onol, Arif Icke, and Orhan Atabay. Strategy optimization of a solar car for a long-distance race using big bang-big crunch optimization. In *Computational Intelligence and Informatics (CINTI), 2013 IEEE 14th International Symposium on*, pages 521–526. IEEE, 2013.

Luis F Zarzalejo, Lourdes Ramirez, and Jesus Polo. Artificial intelligence techniques applied to hourly global irradiance estimation from satellite-derived cloud index. *Energy*, 30(9):1685–1697, 2005.

Richard Zhang, Phillip Isola, and Alexei A Efros. Colorful image colorization. In *European Conference on Computer Vision*, pages 649–666. Springer, 2016.